ARTICLE

De Novo Mutations in Protein Kinase Genes CAMK2A and CAMK2B Cause Intellectual Disability

Sébastien Küry,[1,63,*] Geeske M. van Woerden,[2,3,63] Thomas Besnard,[1,63] Martina Proietti Onori,[2,3] Xénia Latypova,[1] Meghan C. Towne,[4,5] Megan T. Cho,[6] Trine E. Prescott,[7] Melissa A. Ploeg,[2,3] Stephan Sanders,[8] Holly A.F. Stessman,[9,10] Aurora Pujol,[11,12] Ben Distel,[2,3,13] Laurie A. Robak,[14] Jonathan A. Bernstein,[15] Anne-Sophie Denommé-Pichon,[16] Gaëtan Lesca,[17,18] Elizabeth A. Sellars,[19] Jonathan Berg,[20] Wilfrid Carré,[21] Øyvind Løvold Busk,[7] Bregje W.M. van Bon,[22] Jeff L. Waugh,[23] Matthew Deardorff,[24] George E. Hoganson,[25] Katherine B. Bosanko,[19] Diana S. Johnson,[26] Tabib Dabir,[27] Øystein Lunde Holla,[7] Ajoy Sarkar,[28] Kristian Tveten,[7] Julitta de Bellescize,[29] Geir J. Braathen,[7] Paulien A. Terhal,[30] Dorothy K. Grange,[31] Arie van Haeringen,[32]

(Author list continued on next page)

Calcium/calmodulin-dependent protein kinase II (CAMK2) is one of the first proteins shown to be essential for normal learning and synaptic plasticity in mice, but its requirement for human brain development has not yet been established. Through a multi-center collaborative study based on a whole-exome sequencing approach, we identified 19 exceedingly rare de novo CAMK2A or CAMK2B variants in 24 unrelated individuals with intellectual disability. Variants were assessed for their effect on CAMK2 function and on neuronal migration. For both CAMK2A and CAMK2B, we identified mutations that decreased or increased CAMK2 auto-phosphorylation at Thr286/Thr287. We further found that all mutations affecting auto-phosphorylation also affected neuronal migration, highlighting the importance of tightly regulated CAMK2 auto-phosphorylation in neuronal function and neurodevelopment. Our data establish the importance of CAMK2A and CAMK2B and their auto-phosphorylation in human brain function and expand the phenotypic spectrum of the disorders caused by variants in key players of the glutamatergic signaling pathway.

Introduction

Modification of synaptic strength, i.e., synaptic plasticity, is a cornerstone in human capacity to adapt to environmental change. The ability of synapses to modulate their strength is critical for learning and memory processes.[1] Both strengthening (known as long-term potentiation [LTP]) and weakening (known as long-term depression [LTD]) of synaptic transmission have been shown to contribute to distinct types of learning and long-term memory.[2–5]

Abnormal synaptic plasticity is a well-recognized cause of numerous neurological and psychiatric disorders,[6] as exemplified by dysfunctional ionotropic glutamate receptor signaling, notably α-amino-3-hydroxy-5-methyl-4-isoxazole propionic acid receptors (AMPAR) and N-methyl-D-aspartate receptor (NMDAR) signaling.[7–11] For example, pathogenic variants in AMPAR genes GRIA3 (MIM: 305915) (GluA3, associated with mental retardation, X-linked 94 [MIM: 305915])[12,13] and CACNG2 (MIM: 602911) (stargazin, associated with mental retardation, autosomal-dominant 10 [MIM: 614256]),[14] and in genes of NMDAR subunits GRIN1 (MIM: 138249) (GluN1, associated with mental retardation, autosomal-dominant 8 [MIM: 614254]), GRIN2A (MIM: 138253) (GluN2A, associated with focal epilepsy, with speech disorder, and with or without mental retardation [MIM: 245570]), GRIN2B (MIM: 138252) (GluN2B, associated with early infantile epileptic encephalopathy, 27 [MIM: 616139] and mental retardation, autosomal-dominant 6 [MIM: 613970]), and GRIN2D (MIM: 602717) (GluN2D, associated with epileptic encephalopathy, early infantile, 46 [MIM: 617162])[14–20] are a cause of neurodevelopmental disorders.

Another major regulator of synaptic plasticity is the Ca^{2+}/calmodulin-dependent serine/threonine protein kinase CAMK2, whose activation is necessary and

[1]CHU Nantes, Service de Génétique Médicale, 9 quai Moncousu, 44093 Nantes Cedex 1, France; [2]Department of Neuroscience, Erasmus University Medical Center, 3015 CN Rotterdam, the Netherlands; [3]ENCORE Expertise Center for Neurodevelopmental Disorders, Erasmus University Medical Center, 3015 CN Rotterdam, the Netherlands; [4]Division of Genetics and Genomics, Boston Children's Hospital and Harvard Medical School, Boston, MA 02115, USA; [5]Gene Discovery Core, The Manton Center for Orphan Disease Research, Boston Children's Hospital and Harvard Medical School, Boston, MA 02115, USA; [6]GeneDx, Gaithersburg, MD 20877, USA; [7]Department of Medical Genetics, Telemark Hospital Trust, 3710 Skien, Norway; [8]Department of Psychiatry, UCSF Weill Institute for Neurosciences, University of California, San Francisco, San Francisco, CA 94158, USA; [9]Department of Genome Sciences, University of Washington School of Medicine, Seattle, WA 98195, USA; [10]Department of Pharmacology, Creighton University Medical School, Omaha, NE 68178, USA; [11]Neurometabolic Diseases Laboratory, IDIBELL, Gran Via, 199, L'Hospitalet de Llobregat, 08908 Barcelona, and CIBERER U759, Center for Biomedical Research on Rare Diseases, 08908 Barcelona, Spain; [12]Catalan Institution of Research and Advanced Studies (ICREA), 08010 Barcelona, Spain; [13]Department of Medical Biochemistry, Academic Medical Center, University of Amsterdam, 1105AZ Amsterdam, the Netherlands; [14]Department of Molecular and Human Genetics, Baylor College of Medicine, Houston, TX 77030, USA; [15]Department of Pediatrics, Stanford University School of Medicine,

(Affiliations continued on next page)

Christina Lam,[33] Ghayda Mirzaa,[33,34] Jennifer Burton,[25] Elizabeth J. Bhoj,[35,36] Jessica Douglas,[4] Avni B. Santani,[37,38] Addie I. Nesbitt,[37] Katherine L. Helbig,[39,40] Marisa V. Andrews,[31] Amber Begtrup,[6] Sha Tang,[39] Koen L.I. van Gassen,[30] Jane Juusola,[6] Kimberly Foss,[34] Gregory M. Enns,[15] Ute Moog,[41] Katrin Hinderhofer,[41] Nagarajan Paramasivam,[42] Sharyn Lincoln,[4] Brandon H. Kusako,[4] Pierre Lindenbaum,[43,44] Eric Charpentier,[43,44] Catherine B. Nowak,[4] Elouan Cherot,[21] Thomas Simonet,[29] Claudia A.L. Ruivenkamp,[32] Sihoun Hahn,[33] Catherine A. Brownstein,[4,5] Fan Xia,[14,45] Sébastien Schmitt,[1] Wallid Deb,[1] Dominique Bonneau,[16] Mathilde Nizon,[1] Delphine Quinquis,[1] Jamel Chelly,[46,47,48] Gabrielle Rudolf,[47,48,49] Damien Sanlaville,[17,18] Philippe Parent,[50] Brigitte Gilbert-Dussardier,[51] Annick Toutain,[52] Vernon R. Sutton,[45] Jenny Thies,[53] Lisenka E.L.M. Peart-Vissers,[22] Pierre Boisseau,[1] Marie Vincent,[1] Andreas M. Grabrucker,[54,55] Christèle Dubourg,[21] Undiagnosed Diseases Network, Wen-Hann Tan,[4] Nienke E. Verbeek,[30] Martin Granzow,[41] Gijs W.E. Santen,[32] Jay Shendure,[9,60] Bertrand Isidor,[1] Laurent Pasquier,[56] Richard Redon,[43,44] Yaping Yang,[14,45] Matthew W. State,[8] Tjitske Kleefstra,[22] Benjamin Cogné,[1] GEM HUGO[57], Deciphering Developmental Disorders Study[58], Slavé Petrovski,[59] Kyle Retterer,[6] Evan E. Eichler,[9,60] Jill A. Rosenfeld,[14] Pankaj B. Agrawal,[4,5,61] Stéphane Bézieau,[1,62,64] Sylvie Odent,[56,64] Ype Elgersma,[2,3,64,*] and Sandra Mercier[1,64]

sufficient for hippocampal LTP induction.[21] In the hippocampus, CAMK2 forms a dodecameric holoenzyme that is mainly composed of its two predominant subunits, alpha (CAMK2A) and beta (CAMK2B), which together represent 2% of the total hippocampal protein content.[22] The CAMK2A and CAMK2B subunits share a very high degree of homology and consist of four distinct domains: a catalytic domain containing the active site required for CAMK2 kinase activity, a regulatory domain comprising the calcium-calmodulin binding site (including the auto-inhibitory sub-domain of the Thr286/Thr287 phosphorylation site required for autonomous [calcium-independent] activity), a variable domain, i.e., the domain in which CAMK2A and CAMK2B show the largest difference, and an association domain necessary for assembly of the (mixed) holoenzyme with 10–12 CAMK2 subunits.[21,23,24] Subunits combine mainly to form CAMK2A homomers or CAMK2A-CAMK2B heteromers.[2]

Stanford, CA 94305, USA; [16]CHU Angers, Département de Biochimie et Génétique, 49933 Angers Cedex 9, France; UMR INSERM 1083 - CNRS 6015, 49933 Angers Cedex 9, France; [17]Service de génétique, Centre de Référence des Anomalies du Développement, Hospices Civils de Lyon, 69288 Lyon, France; [18]INSERM U1028, CNRS UMR5292, Centre de Recherche en Neurosciences de Lyon, 69675 Bron, France; [19]Section of Genetics and Metabolism, Arkansas Children's Hospital, Little Rock, AR 72202, USA; [20]Molecular and Clinical Medicine, School of Medicine, University of Dundee, Ninewells Hospital & Medical School, Dundee DD1 9SY, UK; [21]Laboratoire de Génétique Moléculaire & Génomique, CHU de Rennes, 35033 Rennes, France; [22]Department of Human Genetics, Nijmegen Center for Molecular Life Sciences, Institute for Genetic and Metabolic Disease, Radboud University Nijmegen Medical Center, 6525 GA Nijmegen, the Netherlands; [23]Department of Neurology, Boston Children's Hospital and Harvard Medical School, Boston, MA 02115, USA; [24]Department of Pediatrics, Division of Genetics, Children's Hospital of Philadelphia, Philadelphia, PA 19104, USA; [25]Department of Pediatrics, University of Illinois at Chicago, College of Medicine, Chicago, IL 60612, USA; [26]Sheffield Children's Hospital, Western Bank, Sheffield S10 2TH, UK; [27]Northern Ireland Regional Genetics Centre, Belfast Health and Social Care Trust, Belfast City Hospital, Lisburn Road, Belfast BT9 7AB, UK; [28]Nottingham Regional Genetics Service, City Hospital Campus, Nottingham University Hospitals NHS Trust, The Gables, Hucknall Road, Nottingham NG5 1PB, UK; [29]Epilepsy, Sleep and Pediatric Neurophysiology Department, Hospices Civils, Lyon, 69677 Bron, France; [30]Department of Genetics, University Medical Center Utrecht, Utrecht 3584 EA, the Netherlands; [31]Division of Genetics and Genomic Medicine, Department of Pediatrics, Washington University School of Medicine, Saint Louis, MO 63110, USA; [32]Department of Clinical Genetics, Leiden University Medical Center (LUMC), 2333 ZA Leiden, the Netherlands; [33]Division of Genetic Medicine, Department of Pediatrics, University of Washington School of Medicine and Seattle Children's Hospital, Seattle, WA 98105, USA; [34]Center for Integrative Brain Research, Seattle Children's Research Institute, Seattle, WA 98101, USA; [35]Center for Applied Genomics, The Children's Hospital of Philadelphia, Philadelphia, PA 19104, USA; [36]Division of Human Genetics, The Children's Hospital of Philadelphia, Philadelphia, PA 19104, USA; [37]Division of Genomic Diagnostics, Department of Path and Lab Medicine, Children's Hospital of Philadelphia, Philadelphia, PA 19104, USA; [38]Department of Path and Lab Medicine, Perelman School of Medicine, University of Pennsylvania, Philadelphia, PA 19104-4238, USA; [39]Division of Clinical Genomics, Ambry Genetics, 15 Argonaut, Aliso Viejo, CA 92656, USA; [40]Division of Neurology, The Children's Hospital of Philadelphia, Philadelphia, PA 19104, USA; [41]Institute of Human Genetics, University Heidelberg, Im Neuenheimer Feld 366, 69120 Heidelberg, Germany; [42]Medical Faculty Heidelberg, Heidelberg University, 69120 Heidelberg, Germany and Division of Theoretical Bioinformatics, German Cancer Research Center (DKFZ), Im Neuenheimer Feld 280, 69120 Heidelberg, Germany; [43]INSERM, CNRS, UNIV Nantes, l'institut du thorax, 44007 Nantes, France; [44]CHU Nantes, l'institut du thorax, 44093 Nantes, France; [45]Baylor Genetics, Houston, TX 77030, USA; [46]Laboratoire de Diagnostic Génétique, Hôpitaux Universitaires de Strasbourg, Nouvel Hôpital Civil, 67091 Strasbourg, France; [47]Fédération de Médecine Translationnelle de Strasbourg (FMTS), Université de Strasbourg, 67000 Strasbourg, France; [48]Institut de Génétique et de Biologie Moléculaire et Cellulaire (IGBMC), INSERM-U964/CNRS-UMR7104/Université de Strasbourg, 67404 Illkirch, France; [49]Service of Neurology, University Hospital of Strasbourg, Hospital of Hautepierre, 1 avenue Molière, 67098 Strasbourg Cedex, France; [50]CHRU Brest, Génétique médicale, 29609 Brest, France; [51]CHU Poitiers, Service de Génétique, BP577, 86021 Poitiers, France; EA 3808 Université Poitiers, France; [52]CHU Tours, Service de Génétique, 2 Boulevard Tonnellé, 37044 Tours, France; [53]Division of Genetic Medicine, Department of Pediatrics, Seattle Children's Hospital, Seattle, WA 98105, USA; [54]Department of Biological Sciences, University of Limerick, Limerick V94 T9PX, Ireland; [55]Bernal Institute, University of Limerick, Limerick V94 T9PX, Ireland; [56]CHU Rennes, Service de Génétique Clinique, CNRS UMR6290, Université Rennes1, 35203 Rennes, France; [57]Réseau de génétique et génomique médicale - Hôpitaux Universitaires du Grand Ouest, CHU Rennes, Service de Génétique Clinique, 35203 Rennes, France; [58]Wellcome Trust Sanger Institute, Wellcome Trust Genome Campus, Hinxton CB10 1SA, UK; [59]Department of Medicine, The University of Melbourne, Austin Health and Royal Melbourne Hospital, Melbourne, VIC 3010, Australia; [60]Howard Hughes Medical Institute, Seattle, WA 98195, USA; [61]Division of Newborn Medicine, Boston Children's Hospital and Harvard Medical School, Boston, MA 02115, USA; [62]CRCINA, Inserm, Université d'Angers, Université de Nantes, 44000 Nantes, France
[63]These authors contributed equally to this work
[64]These authors contributed equally to this work
*Correspondence: sebastien.kury@chu-nantes.fr (S.K.), y.elgersma@erasmusmc.nl (Y.E.)
https://doi.org/10.1016/j.ajhg.2017.10.003.

CAMK2 contributes in various ways to synaptic plasticity, but most critical is its regulation of ionotropic glutamate receptors. In particular, CAMK2 binding to the NMDAR and its ability to regulate the membrane insertion and activity of AMPAR are crucial for regulating synaptic strength.[2,24–26] This process is triggered by Ca^{2+} entry through the NMDAR, resulting in Ca^{2+}/calmodulin binding to the CAMK2 regulatory domain.[24] Subsequent auto-phosphorylation of amino acid residue Thr286 in the inhibitory domain of the α-subunit isoform (or Thr287 in the β-subunit isoform) of CAMK2 allows the enzyme to maintain its activated conformation, thereby effectively converting a very brief Ca^{2+} signal into a long-lasting enzymatic change. Activated CAMK2 translocates from the dendritic shaft to post synaptic densities (PSDs) of dendritic spines, where it binds to NMDAR (GluN1, 2A and 2B) and enhances the insertion and function of AMPAR GluA1 (*GRIA1* [MIM: 138248]), stargazin, and SAP97 (*DLG1* [MIM: 601014])[24] in the PSD. The importance of these events is highlighted by the observation that *Camk2* knock-in mice with mutations interfering with calmodulin binding, or silencing the autonomous or kinetic activity of the protein, result in profound learning and plasticity deficits.[27–29]

Paradoxically, although the *Camk2a* knock-out was the first murine knock-out in the field of neuroscience to establish a critical role for NMDA receptor-mediated calcium signaling in learning and synaptic plasticity,[30,31] the importance of *CAMK2A* (MIM: 114078) for cognitive function has not yet been established. Similarly, *Camk2b* has been shown to be important for learning and synaptic plasticity in mice,[32,33] but mutations in *CAMK2B* (MIM: 607707) have not yet been described. In the present study, we report 19 rare variants in *CAMK2A* or *CAMK2B* in 24 unrelated individuals with intellectual disability (ID), with 23 individuals shown to have *de novo* occurrence of the variants. We also provide evidence that most of these alterations of CAMK2 are likely to affect protein and neuronal function.

Methods

Inclusion of the Individuals and Connection between the Participating Studies

The 24 affected individuals selected in the present study were enrolled together with their healthy parents in 14 different programs or centers investigating the molecular basis of developmental disorders in a research or clinical setting: (1) the Baylor Genetics (BG) Laboratories (Houston, TX, USA; individuals 1 and 16), (2) the Western France consortium HUGODIMS (Projet inter-régional Français des Hôpitaux Universitaires du Grand Ouest pour l'exploration par approche exomique des causes moléculaires de Déficience Intellectuelle isolée ou syndromique Modérée à Sévère; individuals 2 and 7), (3) the Wellcome Trust Sanger Institute British program Deciphering Developmental Disorders (DDD, UK; individuals 3, 14, 18, and 21), (4) the University Medical Center Utrecht (the Netherlands; individuals 4 and 12), (5) the

Simons Simplex Collection (SSC) (USA; individuals 5 and 6), (6) the University Hospital Center (CHU) of Lyon (France; individual 8), (7) Leiden University Medical Center (the Netherlands; individual 9), (8) the Children's Hospital of Philadelphia (USA; individual 10), (9) the Institute of Human Genetics, University Hospital Heidelberg (Germany; individual 11), (10) the Arkansas Children's Hospital, St. Louis Children's Hospital, and Seattle Children's Hospital via GeneDx laboratory (USA; individuals 13, 15, 19, and 22), (10) the Boston Children's Hospital (USA; individual 17), (11) the Undiagnosed Diseases Network (UDN) through the Boston Children's Hospital and Harvard Clinical Site and BG laboratories sequencing site (USA; individual 20), (13) the University of Illinois College of Medicine at Peoria via Ambry Genetics (USA; individual 23), and (14) the Telemark Hospital Trust in Skien (Norway; individual 24). Connecting the 14 centers was facilitated by the web-based tools GeneMatcher[34] and DECIPHER.[35]

In each participating center, clinical assessment was performed by at least one expert clinical geneticist. Routine clinical genetic and metabolic screenings performed during initial workup was negative in each case, which warranted further investigation on a research basis. All families gave written informed consent for inclusion in the study and consent for the publication of photographs was obtained for individuals 3, 7, 15, 16, 17, 22, and 23. The study has been approved by the CHU de Nantes-ethics committee (number CCTIRS: 14.556).

Whole-Exome Sequencing Strategy

Except BG Laboratories, which performed clinical singleton exome sequencing as a first-tier molecular test in individuals 1 and 16, all other centers followed a trio-based approach. Most of the methods used by the centers were detailed previously: HUGODIMS program focused on intellectual disabilities (ID) in 76 trios from simplex families,[36] DDD analyzed more than 4,293 children with severe developmental disorders and their parents,[37] SSC parsed data from 2,508 trios with an autism spectrum disorder,[38] GeneDx laboratory analyzed 11,388 case subjects with ID or developmental disorder (DD) with 8,897 of them being sequenced with both parents and following the method described previously,[39] the Boston Children's Hospital analyzed more than 300 trios including 50 trios with developmental disabilities,[40] the Children's Hospital of Philadelphia sequenced 400 whole exomes (323 trios) including 138 trios with developmental delay that were analyzed according to the method described previously,[41] Ambry Genetics sequenced 2,583 parent-proband trios where the child had childhood-onset neurological disorder applying the strategy described earlier,[42] the University Medical Center Utrecht analyzed the exomes of more than 500 parent-proband trios that were negative after analyzing the gene panel for intellectual disability (~800 known ID genes),[43] the Telemark Hospital Trust in Skien analyzed 531 exomes including 99 trios,[44] Leiden University Medical Center tested 825 exomes including 579 trios with a child presenting ID following a strategy described previously,[45] BG Laboratories queried its internal database of ~5,900 clinical exomes including about 100 trios regarding *CAMK2A* and ~6,400 clinical exomes including about 200 trios regarding *CAMK2B*, which comprised UDN exomes and had been analyzed following clinical diagnostics protocol defined previously,[46,47] and the Institute of Human Genetics, Heidelberg, analyzed trios from 57 families with 63 probands with (neuro) developmental disorders as previously described.[48]

The CHU of Lyon included individual 8 in a cohort of children with typical or atypical Rolandic epilepsy. This last one is among

the most common epileptic syndromes in childhood and may be associated with cognitive impairment or autistic features in a subset of affected children. Individual 8 was recruited in the Department of Epilepsy, Sleep and Pediatric Neurophysiology, at the Lyon University Hospital. The IRB approval number was 05/78, CPP Strasbourg Alsace 1. Exome sequencing was performed with a trio design (in blood DNA from the affected individual and his parents) using in-solution exome capture kits (Sure Select Human All exome 50MB kit, Agilent Technology, or Illumina TruSeq exome Enrichment, Illumina) and Illumina HiSeq sequencing platforms (Illumina) to generate paired end reads sequences (Centre National de Genotypage [CNG], Évry, France).

Following their respective analysis pipelines, participating centers generated a list of candidate variants filtered against public database variants and according to modes of inheritance. Save for families from BG in which *de novo* events in *CAMK2A* and *CAMK2B* were sought post hoc, all other variants reported in the present study were determined independently by participating centers. Candidate variants were confirmed by Sanger capillary sequencing for all but individuals 4, 9, 18, and 21.

Transfection Constructs

The cDNA sequences from human *CAMK2A*^{WT} (GenBank: NM_015981.3) and *CAMK2B*^{WT} (GenBank: NM_001220.4) were obtained from a human brain cDNA library by PCR (Phusion high fidelity, Thermo Fisher) using the following primers: for *CAMK2A* Fw 5′-GAATCCGGCGCGCCACC**ATG**GCCACCATCA CCTGCAC-3′ and Rev 5′-GGATTCTTAATTAA**TCA**GTGGGGCAG GACGGAGG-3′; for *CAMK2B* Fw 5′-GAATCCGGCGCGCCAC C**ATG**GCCACCACGGTGACCTG-3′ and Rev 5′-GGATTCTTAAT TAA**TCA**CTGCAGCGGGGCCACAG-3′ and they were cloned into our dual promoter expression vector (Figure S5). The dual promoter expression vector was generated from the pCMV-*tdTomato* vector (Clontech), where the *CMV* promoter was replaced with a *CAGG* promoter followed by a multiple cloning site (MCS) and transcription terminator sequence. To assure expression of the tdTOMATO independent from the gene of interest, a PGK promoter was inserted in front of the *tdTomato* sequence. For all the *in vivo* and *in vitro* experiments, the vector without a gene inserted in the MCS was taken along as control (control vector).

The different point mutations were introduced with site-directed Mutagenesis (Invitrogen for *CAMK2A*-c.327G>C, *CAMK2A*-c.845A>G, *CAMK2B*-c.328G>A and NEB Q5 Site-Directed Mutagenesis Kit for others) using the following primers: *CAMK2A*-c.293T>C (p.Phe98Ser), Fw 5′-GGGGAACTGTcTGAA GATATCG-3′ and Rev 5′-ACCAGTGACCAGGTCGAA-3′; *CAM K2A*-c.327G>C (p.Glu109Asp), Fw 5′-GGAGTATTACAGTGACG CGGATGCCAGTCAC-3′ and Rev 5′-GTGACTGGCATCCGCGT CACTGTAATACTCC-3′; *CAMK2A*-c.412C>G (p.Pro138Ala), Fw 5′-GGACCTGAAGgCTGAGAATCTGTTG-3′ and Rev 5′-CGGTG CACCACCCCCATC-3′; *CAMK2A*-c.548A>T (p.Glu183Val), Fw 5′-CTCTCCCCAGtAGTGCTGCGG-3′ and Rev 5′-ATATCCAGGA GTCCCTGCAAAC-3′; *CAMK2A*-c.635C>T (p.Pro212Leu), Fw 5′-GGGTACCCCCtGTTCTGGGAT-3′ and Rev 5′-AACCAGCAG GATGTACAGG-3′; *CAMK2A*-c.704C>T (p.Pro235Leu), Fw 5′-TTCCCATCGCtGGAATGGGAC-3′ and Rev 5′-ATCATAGGCG CCGGCTTT-3′; *CAMK2A*-c.845A>G (p.His282Arg), Fw 5′-GG CATCCTGCATGCGCAGACAGGAGACCG-3′ and Rev 5′-CG GTCTCCTGTCTGCGCATGCAGGATGCC-3′; *CAMK2A*-c.856A>C (p.Thr286Pro), Fw 5′-CAGACAGGAGcCCGTGGACTG-3′ and Rev 5′-TGCATGCAGGATGCCACG-3′; *CAMK2B*-c.328G>A

(p.Glu110Lys), Fw 5′-GAGAGAGTACTACAGCAAGGCTGAT GCCAGTCA-3′ and Rev 5′-TGACTGGCATCAGCCTTGCTG TAGTACTCTCTC-3′; *CAMK2B*-c.416C>T (p.Pro139Leu), Fw 5′-GACCTCAAGCtGGAGAACCTG-3′ and Rev 5′-TCTGTGG ACGACCCCCAT-3′; *CAMK2B*-c.709G>A (p.Glu237Lys), Fw 5′-CCCGTCCCCTaAGTGGGACAC-3′ and Rev 5′-AAGTCATA GGCACCAGCC-3′; *CAMK2B*-c.901A>G (p.Lys301Glu), Fw 5′-GA GAAAGCTCgAGGGGAGCCATC-3′ and Rev 5′-CTGGCATTGA ACTTTTTCAGAC-3′. For the control mutations of *CAMK2A*, the different point mutations were introduced with site-directed Mutagenesis (Invitrogen) using the following primers: *CAMK2A*-c.125,126AG>GA (p.Lys42Arg), Fw 5′-GGCCAGGAGTATGCT GCCAGAATCATCAACACAAAGAAGC-3′ and Rev 5′-GCTTCT TTGTGTTGATGATTCTGGCAGCATACTCCTGGCC-3′; *CAMK2A*-c.856-858ACC>GCT (p.Thr286Ala), Fw 5′-ATCGCTATGATGC ATAGACAGGAGGCTGTGGACTGCCTGAAGAAGTTCAAT-3′ and Rev 5′-AGTGTGATGCATGCAGGATGCCACGGTGGAGCGGTGC GAGAT-3′; *CAMK2A*-c.856,857AC>GA (p.Thr286Asp), Fw 5′-AT CGCTATGATGCATAGACAGGAGGACGTGGACTGCCTGAAGAA GTTCAAT-3′ and Rev 5′-AGTGTGATGCATGCAGGATGCCACG GTGGAGCGGTGCGA-3′.

shRNA constructs were obtained from the MISSION shRNA library for mouse genomes of Sigma Life Sciences and The RNAi Consortium (TRC). For knockdown of CAMK2A we had five different shRNA plasmids, each with a different target sequence: (1) GCGTTCAGTTAATGGAATCTT, (2) CCTGGACTTTCATCG ATTCTA, (3) CGCAAACAGGAAATTATCAAA, (4) GCTGATCG AAGCCATAAGCAA, and (5) GTGTTGCTAACCCTCTACTTT. For knockdown of CAMK2B, we had five different shRNA plasmids, each with a different target sequence: (1) CCACCTTGTTATCTC CACAAA, (2) GTACCATCTATACGAGGATAT, (3) CCTGCTGAAG CATTCCAACAT, (4) GACTGTGGAATGTCTGAAGAA, and (5) CTGACCTCATTTGAGCCTGAA. The control shRNA plasmid is the MISSION non-target shRNA control vector: CAACAAGA TGAAGAGCACCAA.

Mice

For the neuronal cultures, FvB/NHsD females were crossed with FvB/NHsD males (both ordered at 8–10 weeks old from Envigo). For the *in utero* electroporation, FvB/NHsD (Envigo) females were crossed with C57Bl6/J males (ordered at 8–10 weeks old from Charles River). All mice were kept group-housed in IVC cages (Sealsafe 1145T, Tecniplast) with bedding material (Lignocel BK 8/15 from Rettenmayer) on a 12/12 hr light/dark cycle in 21°C ($\pm$1°C), humidity at 40%–70% and with food pellets (801727CRM(P) from Special Dietary Service) and water available *ad libitum*. All animal experiments were approved by the Local Animal Experimentation Ethical Committee, in accordance with Institutional Animal Care and Use Committee guidelines.

Cell Culture and Analysis of Protein Stability in Transfected Cells
HEK293T Cell Transfections
We used Thr286/Thr287 auto-phosphorylation as a readout of kinase function. To test the expression vector with the *CAMK2* constructs and to measure the phosphorylation levels of CAMK2, we used a cell line that is easy to transfect and culture, so we chose HEK293T cells. These cells were mycoplasma-free and authenticated (293T-ATCC CRL-3216). HEK293T cells were cultured in DMEM/10% Fetal Calf Serum (FCS)/1% penicillin/streptomycin in 6-well plates and transfected when 50% confluent with the

following DNA constructs: control vector, $CAMK2A^{WT}$, $CAMK2A^{p.(Phe98Ser)}$, $CAMK2A^{p.(Glu109Asp)}$, $CAMK2A^{p.(Pro138Ala)}$, $CAMK2A^{p.(Glu183Val)}$, $CAMK2A^{p.(Pro212Leu)}$, $CAMK2A^{p.(Pro235Leu)}$, $CAMK2A^{p.(His282Arg)}$, $CAMK2A^{p.(Thr286Pro)}$ and $CAMK2B^{WT}$, $CAMK2B^{p.(Glu110Lys)}$, $CAMK2B^{p.(Pro139Leu)}$ and $CAMK2B^{p.(Glu237Lys)}$, and $CAMK2B^{p.(Lys301Glu)}$ (all 3 μg per coverslip). Transfection of the plasmids was done using polyethylenimine (PEI) according to the manufacturer instructions (Sigma). 6–12 hr after transfection, the medium was changed to reduce toxicity. Transfected cells were then used for western blot.

Western Blot

2–3 days after transfection, HEK cells were harvested and homogenized in lysis buffer (10 mM Tris-HCl [pH 6.8], 2.5% SDS, 2 mM EDTA), containing protease inhibitor cocktail (#P8340, Sigma), phosphatase inhibitor cocktail 2 (#P5726, Sigma), and phosphatase inhibitor cocktail 3 (#P0044, Sigma). Protein concentration in the samples was determined using the BCA protein assay kit (Pierce) and then lysate concentrations were adjusted to 1 mg/mL. Western blots were probed with the following primary antibodies: CAMK2A (6G9, 1:40,000, Abcam; validated in Elgersma et al.[27]), CAMK2B (CB-β1, 1:10,000, Invitrogen; validated in van Woerden et al.[49]), ph-Thr286/Thr287 (autophosphorylated CAMK2 antibody; #06-881; 1:1,000; Upstate Cell Signaling Solutions; validated in Elgersma et al.[27]), and RFP (#600401379, 1:2,000, Rockland, validated in this study by overexpression experiments). Secondary antibodies used were goat anti-mouse (#926-32210) and goat anti-rabbit (#926-68021) (all 1:15,000, LI-COR). Blots were quantified using LI-COR Odyssey Scanner and Odyssey 3.0 software. Analysis was done by an experimenter blinded for the transfection conditions.

Testing the Efficiency and Specificity of the shRNA Constructs

Primary Hippocampal Cultures

Primary hippocampal neuronal cultures were prepared from FvB/NHsD wild-type mice according to the procedure described in Banker and Goslin.[50] Briefly, hippocampi were isolated from brains of E16.5 embryos and collected altogether in 10 mL of neurobasal medium (NB, GIBCO) on ice. After two washings with NB, the samples were incubated in pre-warmed trypsin/EDTA solution (Invitrogen) at 37°C for 20 minutes. After 2 times washing in pre-warmed NB, the cells were resuspended in 1.5 mL NB medium supplemented with 2% B27, 1% penicillin/streptomycin, and 1% glutamax (Invitrogen), and dissociated using a 5 mL pipette. After dissociation, neurons were plated in a small drop on poly-D-lysine (25 mg/mL, Sigma)-coated 15 mm glass coverslips at a density of 1×10^6 cells per coverslip in 12-well plates containing 1 mL of supplemented NB for each coverslip. The plates were stored at 37°/5% CO_2 until the day of the transfection.

Neuronal Transfection and Immunocytochemistry

Neurons were transfected after 3 days in vitro (DIV) with a pool of either the CAMK2A shRNAs or CAMK2B shRNAs with an RFP plasmid (Addgene) or the control shRNA with an RFP plasmid (all in total 4 μg per coverslip). Lipofectamine 2000 was used to transfect neurons, according to the manufacturer instructions (Invitrogen). To measure level of knockdown of CAMK2A and CAMK2B, neurons were fixed 5 days post-transfection with 4% paraformaldehyde (PFA)/4% sucrose and stained for CAMK2A or CAMK2B. The following primary antibodies were used: MAP2 (1:500, #188004, Synaptic System, validation can be found

on the manufacturer's website), CAMK2A (6G9, 1:200, Abcam), and CAMK2B (CB-β1, 1:100, Invitrogen). For secondary antibodies, anti-mouse-Alexa488 (#715-545-150) and anti-guinea-pig-Alexa647 (#706-605-148) conjugated antibodies (all 1:200, Jackson ImmunoResearch) were used. Slides were mounted using mowiol-DABCO (Sigma) mounting medium. Confocal images were acquired using a LSM700 confocal microscope (Zeiss).

For the analysis of the protein levels upon shRNA transfection, the "Measure RGB" plugin for ImageJ software was used to measure the intensity of the fluorescent signal of the transfected cell, which was normalized against non-transfected cells on the same coverslip and then normalized against the mean value of control shRNA transfected cells. Analysis was done by an experimenter blinded for the transfection conditions.

Analysis of Neuronal Migration

In Utero Electroporation

The procedure was performed in pregnant FvB/NHsD mice at E14.5 of gestation to target mainly the progenitor cells giving rise to pyramidal cells of the layer 2/3. The DNA construct (1.5–3 μg/μL) was diluted in fast green (0.05%) and injected in the lateral ventricle of the embryos while still in utero, using a glass pipette controlled by a Picospritzer III device. To ensure the proper electroporation of the injected DNA constructs (1–2 μL) into the progenitor cells, five electrical square pulses of 45V with a duration of 50 ms per pulse and 150 ms inter-pulse interval were delivered using tweezer-type electrodes connected to a pulse generator (ECM 830, BTX Harvard Appartus). The electrodes were placed in such a way that the positive pole was targeting the developing somatosensory cortex. The following plasmids were injected: control vector, $CAMK2A^{WT}$, $CAMK2A^{p.(Phe98Ser)}$, $CAMK2A^{p.(Glu109Asp)}$, $CAMK2A^{p.(Pro138Ala)}$, $CAMK2A^{p.(Glu183Val)}$, $CAMK2A^{p.(Pro212Leu)}$, $CAMK2A^{p.(Pro235Leu)}$, $CAMK2A^{p.(His282Arg)}$, $CAMK2A^{p.(Thr286Pro)}$, $CAMK2A^{p.(Thr286Ala)}$, $CAMK2A^{p.(Thr286Asp)}$, $CAMK2A^{p.(Thr286Pro)/p.(Lys42Arg)}$, and $CAMK2B^{WT}$, $CAMK2B^{p.(Glu110Lys)}$, $CAMK2B^{p.(Pro139Leu)}$, $CAMK2B^{p.(Glu237Lys)}$, $CAMK2B^{p.(Lys301Glu)}$ or for knockdown experiments with a pool of the CAMK2A shRNAs with an RFP plasmid (Addgene) or CAMK2B shRNAs with an RFP plasmid, or the control shRNA with an RFP plasmid. After birth, pups (M/F) were sacrificed at P0 for histochemical processing.

Immunohistochemistry

Mice were deeply anesthetized with an overdose of Nembutal and transcardially perfused with 4% paraformaldehyde (PFA). Brains were extracted and post-fixed in 4% PFA. Brains were then embedded in gelatin and cryoprotected in 30% sucrose in 0.1 M phosphate buffer (PB), frozen on dry ice, and sectioned using a freezing microtome (40/50 μm thick). Free-floating coronal sections were washed in 0.1 M PB and a few selected sections were counterstained with 4′,6-diamidino-2-phenylindole solution (DAPI, 1:10,000, Invitrogen) before being mounted with mowiol on glass.

For the migration analysis, at least 9 confocal images (10× objective, 0.5 zoom, 1,024 × 1,024 pixels) were taken from 2–3 non-consecutive sections from at least 3 successfully targeted animals per plasmid. Images were rotated to correctly position the cortical layers, and the number of cells in different layers was counted using ImageJ (Analyze particles option), and the results were exported to a spreadsheet for further analysis. Cortical areas from the pia to the ventricle were divided in 10 equal-sized bins and the percentage of tdTOMATO-positive cells per bin was calculated. To calculate the total percentage of cells that reached the

Table 1. CAMK2A and CAMK2B Mutations Identified in Individuals 1–24

Individual	Geographical Origin	Gene[a]	Chromosomal Position[a]	HGVSc[b]	HGVSp[b]	CADD (Score)[c]	PolyPhen-2 (Score)[d]	Functional Effect[e,f]	Mutation Origin
1	USA	CAMK2A	5:g.149652720del	c.65del	p.Gly22Glufs*10	–	–	LoF[f]	uncertain[g]
2	France	CAMK2A	5:g.149636374A>G	c.293T>C	p.Phe98Ser	17.01	D (1.0)	LoF	de novo
3	UK	CAMK2A	5:g.149636340C>G	c.327G>C	p.Glu109Asp	19.53	D (0.988)	GoF	de novo
4	Netherlands	CAMK2A	5:g.149636332G>A	c.335C>T	p.Ala112Val	32	D (0.999)	ND	de novo
5	USA	CAMK2A	5:g.149631595T>A	c.548A>T	p.Glu183Val	32	D (1.0)	LoF	de novo
6	USA	CAMK2A	5:g.149631543dup	c.598+2dup	p.?	–	–	ND	de novo
7	France	CAMK2A	5:g.149631371G>A	c.635C>T	p.Pro212Leu	35	D (1.0)	uncertain	de novo
8	France	CAMK2A	5:g.149631371G>A	c.635C>T	p.Pro212Leu	35	D (1.0)	uncertain	de novo
9	Netherlands	CAMK2A	5:g.149631371G>A	c.635C>T	p.Pro212Leu	35	D (1.0)	uncertain	de novo
10	USA	CAMK2A	5:g.149630363G>A	c.704C>T	p.Pro235Leu	15.91	D (1.0)	uncertain	de novo
11	Germany	CAMK2A	5:g.149629873C>T	c.817−1G>A	p.?	–	–	ND	de novo
12	Netherlands	CAMK2A	5:g.149629844T>C	c.845A>G	p.His282Arg	27.0	D (1.0)	GoF	de novo
13	USA	CAMK2A	5:g.149629833T>G	c.856A>C	p.Thr286Pro	29.0	D (0.999)	GoF	de novo
14	UK	CAMK2A	5:g.149607754C>T	c.1204+1G>A	p.?	–	–	LoF	de novo
15	USA	CAMK2B	7:g.44323805G>A	c.85C>T	p.Arg29*	35	–	LoF[f]	de novo
16	USA	CAMK2B	7:g.44294154C>T	c.328G>A	p.Glu110Lys	26.3	D (1.0)	GoF	de novo
17	USA	CAMK2B	7:g.44283125G>A	c.416C>T	p.Pro139Leu	20.6	D (1.0)	GoF	de novo
18	UK	CAMK2B	7:g.44283125G>A	c.416C>T	p.Pro139Leu	20.6	D (1.0)	GoF	de novo
19	USA	CAMK2B	7:g.44283125G>A	c.416C>T	p.Pro139Leu	20.6	D (1.0)	GoF	de novo
20	USA	CAMK2B	7:g.44283125G>A	c.416C>T	p.Pro139Leu	20.6	D (1.0)	GoF	de novo
21	UK	CAMK2B	7:g.44281927C>T	c.709G>A	p.Glu237Lys	25.9	D (1.0)	GoF	de novo
22	USA	CAMK2B	7:g.44281383C>T	c.820−1G>A	p.?	–	–	ND	de novo
23	USA	CAMK2B	7:g.44281301T>C	c.901A>G	p.Lys301Glu	22.6	D (0.996)	LoF	de novo
24	Norway	CAMK2B	7:g.44281298C>T	c.903+1G>A	p.?	–	–	ND	de novo

[a]The reference genome used for bioinformatic predictions is GRCh37/hg19.
[b]HGVSc/HGVSp: coding DNA/protein variant described according to the nomenclature HGVS V2.0 established by the Human Genome Variation Society: GenBank: NM_171825.2/NP_741960.1 for CAMK2A and GenBank: NM_172079.2/NP_742076.1 for CAMK2B; nucleotide numbering uses +1 as the A of the ATG translation initiation codon in the reference sequence, with the initiation codon as codon 1.
[c]CADD v1.3 (Phred score): Combined Annotation Dependent Depletion; higher scores are more deleterious.
[d]PolyPhen-2 HumDiv: PolyPhen-2 Human Diversity; D: Probably damaging (≥0.957).
[e]Effect inferred from in vitro experiments; LoF, loss of function; GoF, gain of function; ND, not determined.
[f]Putative effect.
[g]Paternal sample was unavailable.

outer layers of the cortex, the sum of the percentage of targeted cells of bin 1 to 4 was calculated, based on the observation that in the control vectors, the sum of these first four bins corresponded to the outer layers of the cortex. Analysis was done by an experimenter blinded for the transfection conditions.

Structural Modeling

Homology modeling of the CAMK2B was performed using the I-TASSER protein structure prediction server.[51] The protein sequence of the CAMK2B (GenBank: NP_001211.3) without the F-actin binding domain (amino acids 316–504) was submitted as input for structure prediction. The model with the highest confidence (C-score) and topological similarity (Tm-score) was used for structural representation.

Statistical Analysis

All data were assumed to be normally distributed. Statistical difference between each single mutant and its wild-type control for the western blot analyses (stability and phosphorylation) was determined using the two-tailed unpaired t test (dual comparison), since each mutation was tested against its own wild-type control. For the in vitro knock-down experiments, statistical difference was assessed using one-way ANOVA followed by Dunnet's multiple comparison test.

For the in vivo experiments on neuronal migration, the analysis was performed on the amount of targeted cells (measured as area under the curve) of the first four bins, considered to correspond to the layers 2/3 of the somatosensory cortex. Statistical analysis was performed using one-way ANOVA, followed by Bonferroni's multiple comparison tests. Based on previous experiments
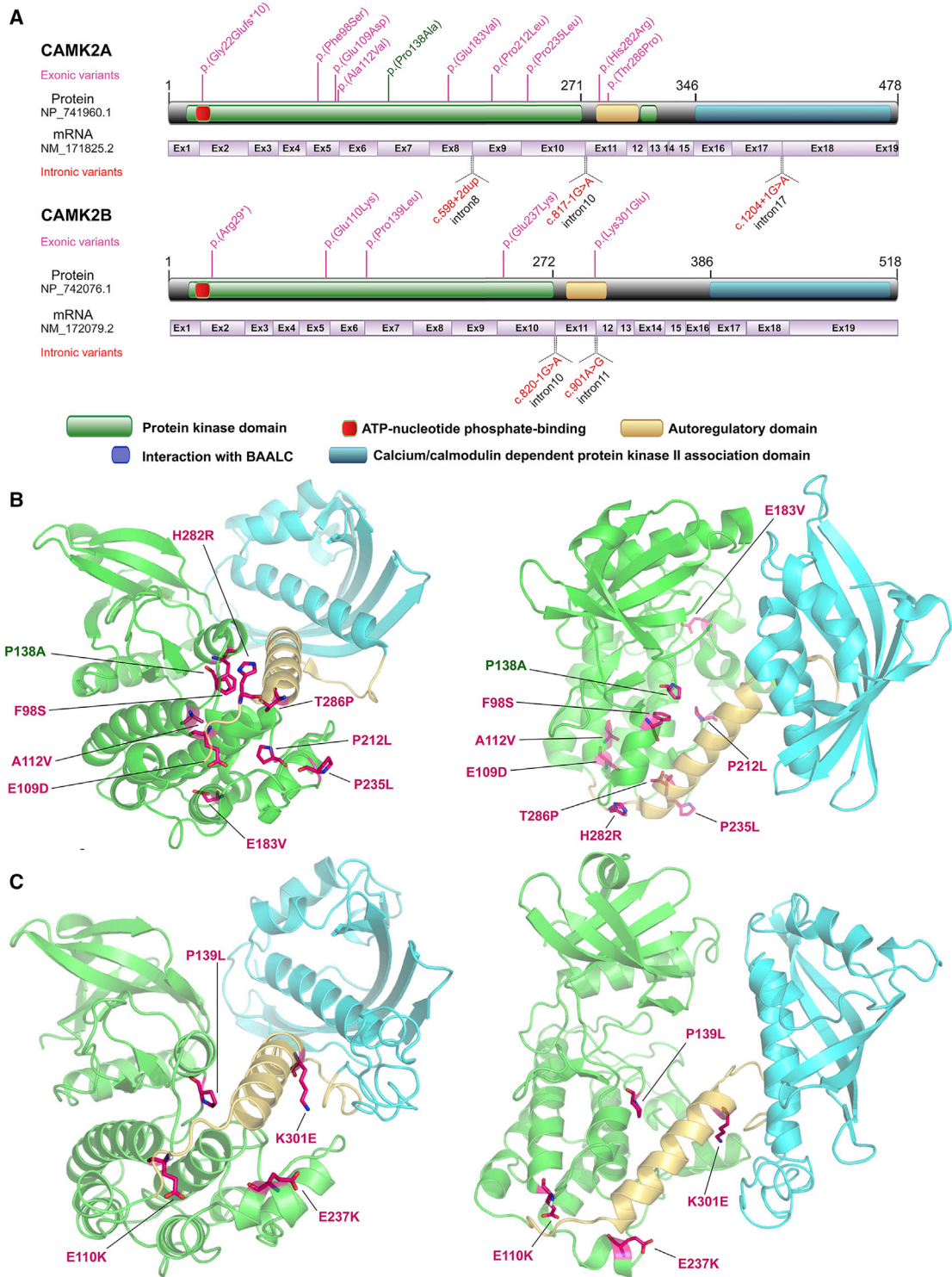
Figure 1. Molecular Genetic Findings in Individuals with *CAMK2A* and *CAMK2B* Variants

(A) Schematic of CAMK2A and CAMK2B protein domain organizations and corresponding mRNA structure (derived from PDB features for Q9UQM7 and Q13554) indicating the positions of 12 missense variants, 1 stop-gain variant, 1 frameshift deletion, and 5 splice site variants found in affected individuals, together with the variant CAMK2A p.Pro138Ala reported in the literature as *de novo*.[38,52]

(B and C) Representation of the structure of a single human CAMK2A subunit obtained from the corresponding full-length holoenzyme structure present in the protein data bank (PDB ID: 3SOA) (B) and homology model of a single human CAMK2B subunit without the F-actin binding domain (C). For both structures, the catalytic domain is represented in green, the autoregulatory domain in yellow, and the association domain in cyan. The location of each single point variant (in magenta) in CAMK2A and CAMK2B, respectively, is indicated in the 3D structure (two different orientations), showing that for CAMK2A seven of the missense variants are located in the catalytic domain, and two variants in the autoregulatory domain. No variants were found in the association domain (B). For CAMK2B, three of the missense variants are located in the catalytic domain and one in the autoregulatory domain. No variant was found

(legend continued on next page)

performed in our lab, we considered that for the knock-down experiments *in vitro*, at least 10 neurons were necessary. For the western blot analysis, we considered at least 3 replicates, and for the IUE experiments, previous experiments in our laboratory showed that at least 3 targeted pups and a minimum of 2 pictures from different brain slices per pup were necessary to draw any conclusion about the migration. Data are represented as box and whisker plots with the minimum and maximum of all the data and p values less than 0.05 are considered significant. All the data were analyzed using the graphpad prism 6.0 software.

Results

Distribution of the Variants in *CAMK2A* and *CAMK2B*

Nineteen different heterozygous variants in *CAMK2A* or *CAMK2B* were identified in 24 unrelated individuals with ID (Table 1). The *de novo* status of these was confirmed for 18 of the 19 variants; it could not be confirmed in individual 1, whose paternal DNA sample was unavailable. The vast majority of the distinct variants—eight in *CAMK2A* and four in *CAMK2B* (Figure 1 and Table 1)—are missense substitutions; eight of the missense variants are predicted to affect the catalytic domain of the protein and the remainder to affect the regulatory domain (Figure 1). Two variants, one in *CAMK2A* and the other in *CAMK2B*, induce the production of mRNA transcripts with a premature stop codon. These transcripts are either eliminated by nonsense-mediated mRNA decay (NMD) or result in a severely truncated and non-functional protein (Figure 1 and Table 1). According to ExAC, the probability of being loss-of-function (LoF) intolerant (pLI) is high for *CAMK2A* (pLI = 1) but lower for *CAMK2B* (pLI = 0.47). However, when one takes into account only the LoF variants observed in the most abundant transcript in brain, GenBank: NM_172079.2 (Ensembl: ENST00000457475), pLI increases to 1 (Figure S9). In the context of a neurodevelopmental disorder, it suggests that *CAMK2B* is also intolerant to LoF variants. The five remaining variants affect canonical splice sites (Table 1), according to bioinformatic predictions and *in vitro* assessment by mini-gene system: three of them would induce skipping of in-frame exons encoding a part of the CAMK2A kinase domain or the entire CAMK2B regulatory domain, while the fourth variant would entail loss of most of the CAMK2 association domain by out-of-frame skipping of exon 17 (Figure S3).

Except variants c.635C>T (p.Pro212Leu) and c.704C>T (p.Pro235Leu), which were deposited in dbSNP, all variants are absent in available public databases (Table S4) and represent the only confirmed *de novo* events in *CAMK2* genes in more than 68,123 in-house exomes, including 19,980 complete trios whose proband had developmental delay of unknown etiology. Individual 10's variant c.704C>T (p.Pro235Leu) was assigned dbSNP accession number rs864309606 (with no frequency) after its submission to ClinVar under accession number SCV000258098; to our knowledge it was reported in no other study than the present one. With respect to variant rs926027867 (p.Pro212Leu) (not validated; no frequency in dbSNP), it was batch-submitted from the large project HUMAN_LONGEVITY|HLI-5-150251808-G-A. Because the phenotype of the individuals from this cohort is not documented, it is possible that the individual carrying variant p.Pro212Leu has intellectual disability.

The variants identified affect amino acids that are highly conserved across CAMK2 paralogs (Figure S4) and species, and are predicted to be likely pathogenic by the majority of bioinformatic programs tested (Table S4); for instance, all variants are predicted to belong to the 5% to 0.05% most deleterious substitutions in the human genome (CADD PHRED score between 16 and 35; Table S4).

Recurrence is noted for two variants located at CpG sites: *CAMK2A* c.635C>T (p.Pro212Leu; n = 3 unrelated individuals) and *CAMK2B* c.416C>T (p.Pro139Leu; n = 4 unrelated individuals) (Table S4). Strikingly, homologous amino acid residues Glu109 in CAMK2A and Glu110 in CAMK2B are altered in two individuals (c.327G>C [p.Glu109Asp] in individual 3 and c.328G>A [p.Glu110Lys] in individual 16). The two *CAMK2B* splice site variants c.820−1G>A and c.903+1G>A affect the canonical splice sequence and are predicted to lead to in-frame skipping of exon 11 according to bioinformatic predictions and *in vitro* studies (Figure S3). Their homologous counterpart in *CAMK2A*, c.817−1G>A, is predicted to have a similar consequence on CAMK2A exon 11 (Figure S3).

We used denovolyzeR[53] to determine whether the 23 *de novo* variants found among our case subjects could have been found by chance given the number of case-ascertained trios studied. Based on the collection of 19,980 trios, and accounting for a gene's underlying mutability, the probability of seeing 13 non-synonymous *CAMK2A de novo* variants by chance is $p = 1.7 \times 10^{-11}$ and $p = 3.9 \times 10^{-8}$ for observing 10 *CAMK2B* non-synonymous *de novo* variants by chance. Both these signals are genome-wide significant after correction for the ~19,000 protein-coding genes where an enrichment could have been found (adjusted $\alpha = 2.6 \times 10^{-6}$). Furthermore, we found that the case missense *de novo* variants within our series were preferentially affecting the most missense intolerant sequence of these two genes. We compared the missense tolerance ratio (MTR) scores[54] of the 17 *CAMK2A* and *CAMK2B de novo* missense variants to 39 rare *CAMK2A* and *CAMK2B* missense variants found among the DiscovEHR cohort of approximately 50,000 control individuals that do not overlap with the gnomAD

in the association domain (C). Structure representations were made with PyMol. Correspondence between the nomenclatures of amino acid changes: F98S, p.Phe98Ser; G109D, p.Glu109Asp; A112V, p.Ala112Val; P138A, p.Pro138Ala; E183V, p.Glu183Val; P212L, p.Pro212Leu; P235L, p.Pro235Leu; H282R, p.His282Arg; T286P, p.Thr286Pro; E110K, p.Glu110Lys; P139L, p.Pro139Leu; E237K, p.Glu237Lys; K301E, p.Lys301Glu.

Table 2. Main Clinical Features of the Individuals with *CAMK2A* and *CAMK2B* Mutations Summarized using Human Phenotype Ontology (HPO) Terms

Clinical Feature	1	2	3	4	5	6	7	8	9	10	11
Intellectual disability (HP:0001249)	+ mod.	+ mod.	+ sev.	+ sev.	+ mild	+ sev.	+ sev.	+ mild/sev.	+ mod.	+ mild	+ sev.
Delayed speech and language development (HP:0000750)	+	+	+	+	+	+	+	+	+	+	+
Abnormal emotion/affect behavior (HP:0100851)	+	+	+	+	+	+	−	+	+	+	+
Global developmental delay (HP:0001263)	+	+	+	+	+	+	+	+	+	−	+
Delayed gross motor development (HP:0002194)	+	+	+	+	+	+	+	+	+	−	+
Hypotonia (HP:0001252)	−	+	+	+	−	−	+	+	−	−	+
Abnormal facial shape (HP:0001999)	+	+	+	−	−	−	+	−	−	+	−
Abnormality of the digestive system (HP:0025031)	−	−	−	−	−	−	−	−	−	−	+
Growth abnormality (HP:0001507)	−	−	−	−	−	−	+	−	−	+	−
Visual impairment (HP:0000505)	−	−	−	−	−	−	−	−	−	−	+
Seizures (HP:0001250)	−	−	+	−	−	−	+	+	−	−	+
EEG abnormality (HP:0002353)	ND	ND	−	−	ND	−	−	+	−	ND	+
Microcephaly (HP:0000256)	−	−	−	−	−	−	−	−	−	−	+

Abbreviations: mod, moderate; sev, severe; ND, not determined.

dataset. Remarkably, 16/17 (94%) of our case missense *de novo* variant events and 12/39 (31%) of the novel control missense variants affect the 50% most missense intolerant sequence of these two genes, as defined by the MTR (Figure S10; Fisher's exact test p = 1.8×10^{-5}; OR 33.7 [95% CI 4.3–1,549.4]).

In addition to the 19 distinct *de novo* variants, we extended our functional investigations to *CAMK2A* c.412C>G (p.Pro138Ala), reported as a *de novo* event in an individual showing severe global developmental delay with seizures (S.E. Holder, personal communication) from a large cohort study.[52] Interestingly, this variant lies in the region encoding the kinase domain, within the most missense-depleted sequence of *CAMK2A* (Figure S10). It is predicted as pathogenic by bioinformatic programs (Table S4) and affects amino acid P138, which is homologous to CAMK2B residue Pro139 altered by variant p.Pro139Leu found in individuals 17–20.

Phenotypic Characterization of Individuals with *CAMK2A* and *CAMK2B* Variants

CAMK2A/B variants cause a neurodevelopmental disorder associated with ID. The main clinical features of affected individuals are summarized in Table 2 using Human Phenotype Ontology terms. More detailed observations are described in Supplemental Note: Case Reports and Tables S1 and S2. Key features are ID, language impairment, and behavioral anomalies. All individuals (24/24) have mild to severe ID. Impaired language development is frequently associated (23/24) with severe delayed speech (first words after age of 3 in 13/21 and no speech or few words after 5 years in 12/15). Epilepsy is reported in 7/23 (absence, febrile, Rolandic, or tonic-clonic seizures). Behavioral issues (19/24) include irritability, low tolerance to frustration, hyperactivity, anxiety, aggressiveness, or autistic traits. Brain imaging was generally normal (mild corpus callosum anomalies in 3/21). The recurrent extra-neurological anomalies include facial dysmorphism (11/24; e.g., hypotelorism, down-slanting palpebral fissures, and epicanthus), visual problems (9/24, including 7/10 in subjects found with a *CAMK2B* variant; e.g., strabismus [4/24], visual impairment, and visual tracking difficulty), gastro-intestinal issues (8/21; e.g., feeding difficulties, reflux, and constipation; 7/9 related to *CAMK2B* variants versus 1/12 related to *CAMK2A*), breathing irregularities (2/24), and scoliosis (2/24). A few features tend to differ between the *CAMK2A*- and the *CAMK2B*-associated groups, although the robustness of the comparison is based on a relatively small sample size (Table S2). Cognitive impairment seems more severe when caused by *CAMK2B* variants, with severe or mild-to-moderate ID present in 8 of 10 individuals with *CAMK2B* variants and 8 of 14 individuals with *CAMK2A* variants. Similarly, hypotonia is more predominant in the *CAMK2B* subgroup (9/10, 90%) than in the *CAMK2A* subgroup (7/14, 50%). When CAMK2A and CAMK2B variants are taken together, ID appears to be more severe when variants affect the autoregulatory domain (6/6) compared to the kinase domain (10/17).

12	13	14	15	16	17	18	19	20	21	22	23	24	Occurrence
+ sev.	+ sev.	+ mild	+ mild	+ mild	+ sev.	+ sev.	+ sev.	+ severe	+ sev.	+ sev.	+ sev.	+ mild/sev.	24/24 (100%)
+	+	−	+	+	+	+	+	+	+	+	+	+	23/24 (95.8%)
+	−	+	−	+	+	+	+	−	+	−	+	+	19/24 (79.2%)
+	+	−	−	+	+	+	+	+	+	+	−	+	19/24 (79.2%)
+	+	−	−	−	+	+	+	+	+	+	−	+	19/24 (79.2%)
−	+	−	−	+	+	+	+	+	+	+	+	+	16/24 (66.7%)
−	−	−	−	−	+	+	+	+	+	−	+	−	11/24 (45.8%)
ND	−	+	−	+	+	+	+	+	+	+	−	+	10/23 (43.5%)
−	−	−	−	−	+	+	+	+	+	−	+	+	9/24 (37.5%)
−	−	+	−	+	+	+	+	+	−	+	−	+	9/24 (37.5%)
−	−	−	+	−	−	−	−	−	+	−	+	+	8/24 (33.3%)
−	ND	ND	ND	+	−	−	ND	ND	+	−	+	+	6/15 (40.0%)
−	−	−	−	−	+	−	+	+	−	−	+	+	6/24 (25.0%)

CAMK2A and CAMK2B Mutations Can Affect Protein Expression

Missense variants were tested using in vitro and in vivo assays to understand their possible effect on protein stability and function (Figure 2A).

Confirming a recent study showing that the CAMK2A[p.(Glu183Val)] variant renders CAMK2A unstable both in vitro and in vivo,[55] transfection of HEK293T cells with the CAMK2A[p.(Glu183Val)] mutant construct showed a significant reduction of CAMK2A protein level compared to CAMK2A[WT] (for all statistics, see Table 3) (Figure 2B). Of the additional seven variants tested, the CAMK2A[p.(His282Arg)] variant also resulted in reduced CAMK2A protein levels after transfection in HEK293T cells, whereas CAMK2A[p.(Phe98Ser)], CAMK2A[p.(Glu109Asp)], CAMK2A[p.(Pro138Ala)], CAMK2A[p.(Pro212Leu)], CAMK2A[p.(Pro235Leu)], and CAMK2A[p.(Thr286Pro)] did not affect CAMK2A protein levels (Table 3 and Figure 2C). Variants CAMK2B[p.(Glu110Lys)] and CAMK2B[p.(Pro139Leu)] showed reduced CAMK2B protein levels (Table 3 and Figure 2C).

Mutations in CAMK2 Have Heterogeneous Effects on CAMK2 Auto-phosphorylation

CAMK2A auto-phosphorylation at Thr286 is critical for autonomous (calcium-independent) function.[28] We therefore investigated how the variants affect Thr286 (CAMK2A) and Thr287 (CAMK2B) auto-phosphorylation. We found that CAMK2A[p.(Glu109Asp)] as well as CAMK2A[p.(His282Arg)] despite reduced protein levels, showed a significant increase in phosphorylation at Thr286 when compared to CAMK2A[WT]. In contrast, CAMK2A[p.(Phe98Ser)] and CAMK2A[p.(Glu183Val)] showed a significant reduction of Thr286 phosphorylation (Table 3 and Figure 2D), the latter being again consistent with a recent study of Camk2a[p.(Glu183Val)] knock-in mice.[55] As expected, we found no phosphorylation at Thr286 when overexpressing CAMK2A[p.(Thr286Pro)] in HEK293T cells underscoring the specificity of the antibody. CAMK2A[p.(Pro138Ala)], CAMK2A[p.(Pro212Leu)], and CAMK2A[p.(Pro235Leu)] showed similar levels of Thr286 phosphorylation compared to CAMK2A[WT] (Table 3 and Figure 2D). We observed nearly abolished Thr287 phosphorylation of the CAMK2B[p.(Lys301Glu)] protein, whereas the CAMK2B[p.(Glu110Lys)], CAMK2B[p.(Pro139Leu)], and CAMK2B[p.(Glu237Lys)] proteins showed a significant increase in phosphorylation at Thr287 (Table 3 and Figure 2E).

Taken together, these results indicate that the identified CAMK2A and CAMK2B variants can exert very diverse effects on CAMK2 auto-phosphorylation.

CAMK2A and CAMK2B Mutations that Affect Auto-phosphorylation also Affect Neuronal Function

Neuronal migration is a key aspect of cortical development. The ability of neurons to migrate from the subventricular zone to layer 2/3 of the somatosensory cortex is highly sensitive to changes that perturb normal neuronal function, resulting in migration deficits.[56–58] Hence, we used in utero electroporation of E14.5 mouse embryos to transfect neurons in the subventricular zone to study the functional effects of variants in CAMK2A and CAMK2B.
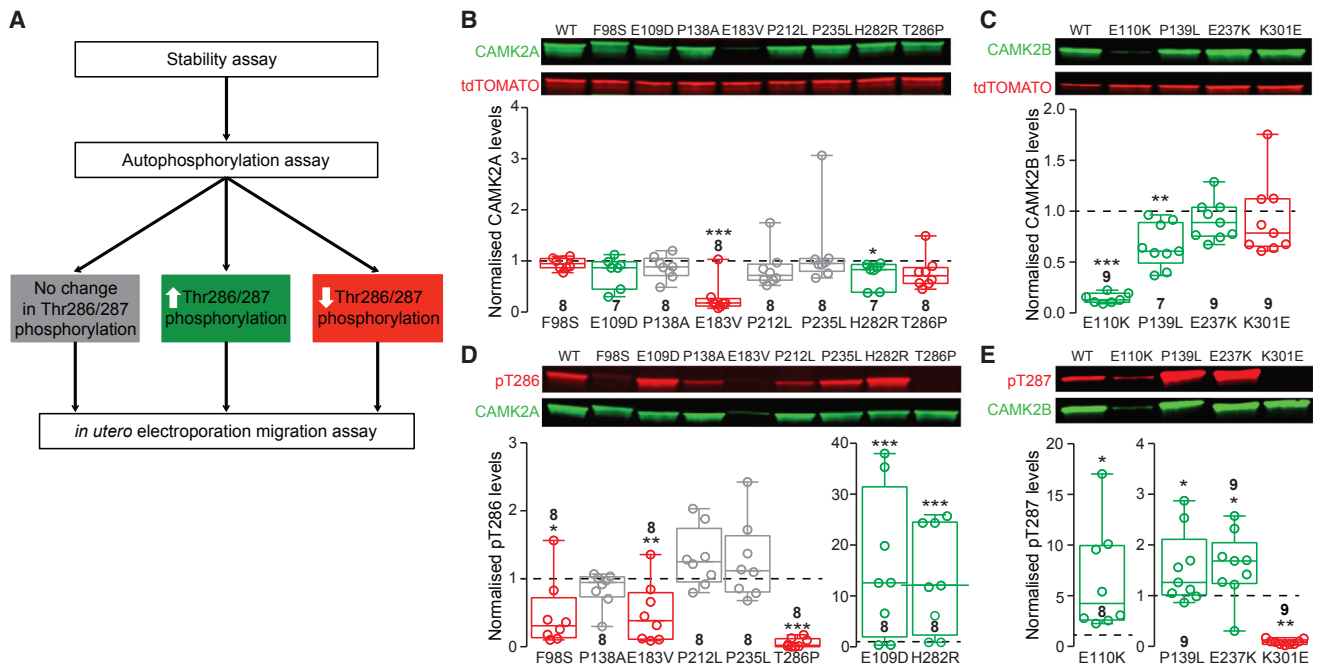
Figure 2. Transfection of HEK293T Cells with the Different CAMK2 Mutants Shows Changes in Stability as well as Phosphorylation at Thr286/287

(A) Schematic overview of the *in vitro* and *in vivo* assays.

(B and C) Top, Representative western blots of HEK293T cells transfected with either *CAMK2A* or *CAMK2B* constructs, probed with an antibody against CAMK2A, CAMK2B, and RFP. Below, quantification of the normalized protein levels of CAMK2A or CAMK2B, showing instability for CAMK2A[p.(Glu183Val)], CAMK2A[p.(His282Arg)], CAMK2B[p.(Glu110Lys)], and CAMK2B[p.(Pro139Leu)] proteins.

(D and E) Top, Representative western blots of HEK293T cells transfected with either *CAMK2A* or *CAMK2B* constructs, probed with a specific antibody against the phosphorylation site Thr286/287 and an antibody against CAMK2A and CAMK2B, respectively. Below, quantification of the normalized levels of CAMK2A-Thr286 phosphorylation and normalized levels of CAMK2B-Thr287 phosphorylation.

Number in the box and whisker plot graphs indicates the n per construct. Error bars indicate the minimum and maximum of all data. Individual data points are shown in the box and whisker plots. Correspondence between the nomenclatures of amino acid changes: F98S, p.Phe98Ser; G109D, p.Glu109Asp; A112V, p.Ala112Val; P138A, p.Pro138Ala; E183V, p.Glu183Val; P212L, p.Pro212Leu; P235L, p.Pro235Leu; H282R, p.His282Arg; T286P, p.Thr286Pro; E110K, p.Glu110Lys; P139L, p.Pro139Leu; E237K, p.Glu237Lys; K301E, p.Lys301Glu.

We first assessed whether reduced or increased levels of (wild-type) CAMK2A and CAMK2B affect neuronal function. Neither increasing nor reducing CAMK2A expression levels affected neuronal migration, whereas changing the protein level of CAMK2B in either direction resulted in clear migration deficits (Tables 4 and 5 and Figures 3A–3C). For efficiency and specificity of the shRNAs used, see Figure S6. These differences may reflect the presence of a unique F-actin binding domain in CAMK2B, which is required to target the entire CAMK2 holoenzyme to the F-actin cytoskeleton.[59] Moreover, CAMK2B is the predominant CAMK2 isoform of the developing brain.[60]

We next electroporated the different mutant *CAMK2* constructs and analyzed their effects on neuronal migration. Even though overexpression or knockdown of CAMK2A did not affect migration, overexpression of CAMK2A mutants with reduced (CAMK2A[p.(Phe98Ser)] and CAMK2A[p.(Glu183Val)]) or increased (CAMK2A[p.(Glu109Asp)] and CAMK2A[p.(His282Arg)]) Thr286 phosphorylation systematically showed reduced migration when compared to overexpression of CAMK2A[WT] (Tables 4 and 5 and Figures 4A, 4C, and 4D). These results strongly suggest that these variants

exert a dominant change of function on the CAMK2 holoenzyme. Conversely, overexpression of the mutant CAMK2A proteins that did not show any effect on Thr286 phosphorylation (CAMK2A[p.(Pro138Ala)], CAMK2A[p.(Pro212Leu)], and CAMK2A[p.(Pro235Leu)]) (Figure 2C) also did not affect migration (Tables 4 and 5 and Figures 4A and 4B). Notably, overexpression of the CAMK2A[p.(Thr286Pro)] mutant completely blocked neuronal migration (Figures 5A and 5B). Since this variant destroys the Thr286 phosphorylation site, it is conceivable that this dramatic effect on migration is caused by severely reduced CAMK2A activity. However, when testing CAMK2A[p.(Thr286Ala)] (phospho-dead CAMK2A mutant)[27,28] and CAMK2A[p.(Thr286Asp)] (phosphomimetic CAMK2A mutant),[61,62] only the latter mimicked the migration pattern found in the CAMK2A[p.(Thr286Pro)] mutant (Figures 5A and 5C). These results indicate that, even though the CAMK2A[p.(Thr286Pro)] cannot be auto-phosphorylated at the Thr286 site, the variant likely functions as a phosphomimetic mutation, resulting in a gain of function. To further test this hypothesis, we introduced a second variant in the CAMK2A[p.(Thr286Pro)] mutant, the p.Lys42Arg variant, which blocks all kinase activity.[29] We found that overexpression

Table 3. Overview of the Statistical Analysis on the Western Blot Experiments for Stability and Thr286/7 Phosphorylation

	Stability			Thr286/7 Phosphorylation		
	p value	df	t-value	p value	df	t-value
CAMK2A						
WT versus p.(Phe98Ser)	0.19	14	1.36	0.01*	14	2.98
WT versus p.(Glu109Asp)	0.06	13	2.02	0.01*	14	2.87
WT versus p.(Pro138Ala)	0.12	14	1.63	0.13	14	1.62
WT versus p.(Glu183Val)	<0.0001*	14	6.56	0.0006*	14	3.23
WT versus p.(Pro212Leu)	0.29	14	1.11	0.06	14	2.03
WT versus p.(Pro235Leu)	0.53	14	0.64	0.23	14	1.27
WT versus p.(His282Arg)	0.01*	13	2.99	0.004*	14	3.35
WT versus p.(Thr286Pro)	0.07	14	1.98	<0.0001*	14	39.23
CAMK2B						
WT versus p.(Glu110Lys)	<0.0001*	14	52.11	0.006*	15	3.21
WT versus p.(Pro139Leu)	0.0002*	16	4.78	0.03*	16	2.32
WT versus p.(Glu237Lys)	0.18	16	1.39	0.02*	16	2.66

Statistical test performed is the two-tailed unpaired t test. Asterisks (*) indicate statistical significant difference.

of the CAMK2A$^{p.(Thr286Pro)/p.(Lys42Arg)}$ protein no longer caused a major delay in migration (Figures 5A and 5D), further confirming that the CAMK2A$^{p.(Thr286Pro)}$ variant acts as gain-of-function variant. Taken together, these results highlight the importance of tightly controlled CAMK2A-Thr286 auto-phosphorylation for normal neuronal function and are consistent with the observation that Thr286 mutations that either abolish auto-phosphorylation or mimic auto-phosphorylation impair synaptic plasticity and learning.[28,62]

Although overexpression of CAMK2B^{WT} affects neuronal migration, we found that overexpression of CAMK2B$^{p.(Glu110Lys)}$, CAMK2B$^{p.(Pro139Leu)}$, or CAMK2B$^{p.(Glu237Lys)}$ disrupted migration even more severely (Tables 4 and 5 and Figures 6A–6C). This is entirely in line with the finding that these three variants result in increased activity as judged by Thr287 auto-phosphorylation (Figure 2E). Overexpression of CAMK2B$^{p.(Lys301Glu)}$, which displays reduced CAMK2 activity (Figure 2E), showed a less severe migration deficit compared to overexpression of CAMK2B^{WT} (Tables 4 and 5 and Figures 5A–5C), indicating that this variant alleviates the deleterious effect of CAMK2B overexpression. Hence, similarly to CAMK2A mutations, these results indicate that all CAMK2B missense mutations that affect Thr287 auto-phosphorylation exert a dominant effect, regardless of whether phosphorylation is increased or decreased.

Discussion

The first mouse mutant with impaired learning and memory was reported 25 years ago when the Camk2a knock-out

was shown to have impaired hippocampus-dependent learning and impaired hippocampal synaptic plasticity.[30,31] Subsequently, an overwhelming amount of data has highlighted the importance of CAMK2A and CAMK2B for many brain areas.[2,21,63] The regulation of kinase activity by auto-phosphorylation has been demonstrated to be essential for the role of CAMK2 in murine neuronal function.[2,28,62] We now provide evidence that proper CAMK2A and CAMK2B functioning is also important for the human brain. We report 24 individuals with a neurodevelopmental disorder who carry a rare heterozygous nonsense, missense, or splice site variant in CAMK2A or CAMK2B—the majority (23/24) were proven de novo. The core clinical findings in affected heterozygous individuals are neurological and consistent with the knockout mouse models for Camk2a and Camk2b[30,32,64,65] (the majority of which are homozygous knock-out). Variants in CAMK2A or CAMK2B result in a non-dysmorphic neurodevelopmental phenotype characterized by a variable degree of ID. Language development is particularly impaired and behavioral problems are frequent. In our cohort, motor delay was more pronounced in the subgroup of individuals with CAMK2A variants, while ID appeared to be more severe and more frequently accompanied by hypotonia with CAMK2B variants. The differential diagnosis of the CAMK2A/B-associated disorder includes many individually rare neurodevelopmental disorders and is virtually impossible to diagnose without molecular testing.

A number of molecular arguments helped us to draw an outline of the clinical entity caused by CAMK2A or CAMK2B variants. The 23 proven de novo events reported here occur in two genes bioinformatically predicted to be intolerant to functional variations (Table S4). They are

Table 4. Overview of the Statistical Analysis on the In Utero Electroporation Experiments: Sum Percentage Targeted Cells Bin 1–4 (One-way ANOVA)

	p value	F
shRNA	<0.0001*	(2,22) 53.58
CAMK2 WT	<0.0001*	(2,23) 17.70
CAMK2A	<0.0001*	(3,24) 51.07
CAMK2B	<0.0001*	(4,38) 17.54
CAMK2A controls mutants	<0.0001*	(3,24) 51.07

Asterisks (*) indicate statistical significant difference.

Table 5. Post-hoc Analysis of the In Utero Electroporation Experiments: Sum Percentage Targeted Cells Bins 1–4 (Bonferroni's Multiple Comparison Test)

	p Value
shRNA	
ctr versus CAMK2A	0.7
ctr versus CAMK2B	<0.0001*
CAMK2 WT	
ctr versus CAMK2A	0.07
ctr versus CAMK2B	<0.0001*
CAMK2A	
WT versus p.Phe98Ser	0.36
WT versus p.Glu109Asp	<0.0001*
WT versus p.Pro138Ala	0.99
WT versus p.Glu183Val	0.002*
WT versus p.Pro212Leu	0.99
WT versus p.Pro235Leu	0.99
WT versus p.His282Arg	<0.0001*
WT versus p.Thr286Pro	<0.0001*
CAMK2B	
WT versus p.Glu110Lys	0.008*
WT versus p.Pro139Leu	0.0007*
WT versus p.Glu237Lys	0.005*
WT versus p.Lys301Glu	0.019*
shRNA	
WT versus p.Thr286Ala	0.002*
WT versus p.Thr286Asp	<0.0001*
WT versus p.Thr286Pro/p.Lys42Arg	0.02*

Asterisks (*) indicate statistical significant difference.

the only such events in the *CAMK2* genes noted in 19,980 trios. The extremely rare variants were identified in individuals who shared the same main clinical phenotype, making it unlikely that they represent incidental findings. The probability of observing 13 or more *CAMK2A* and 10 or more *CAMK2B* non-synonymous *de novo* variants by chance among 19,980 trios is extremely low (*CAMK2A* $p = 1.7 \times 10^{-11}$ and *CAMK2B* $p = 3.9 \times 10^{-8}$), implicating *CAMK2A* and *CAMK2B* as genome-wide significant developmental delay associated genes (exome-wide multiplicity adjusted $p < 2.6 \times 10^{-6}$).

In order to test this assumption further, we employed a number of functional assays to investigate the pathogenicity of the *CAMK2A/B* missense variants. We analyzed their effect on protein stability, Thr286/Thr287 (auto) phosphorylation, and neuronal function by using a neuronal migration assay. Whereas overexpression or knockdown of CAMK2A does not lead to aberrant migration, we found that five out of eight tested missense variants (CAMK2A[p.(Phe98Ser)], CAMK2A[p.(Glu109Asp)], CAMK2A[p.(Glu183Val)], CAMK2A[p.(His282Arg)], and CAMK2A[p.(Thr286Pro)]) affect neuronal migration when expressed *in vivo*. Notably, all these mutants showed either increased or decreased Thr286 phosphorylation in our cellular assays. Auto-phosphorylation of the Thr286 residue has been shown to be essential for CAMK2A function: it renders the protein autonomously active and facilitates interaction with the carboxy-terminal region of GRIN2B (GluN2B) NMDAR subunit.[2,3,66] Based on our results we further conclude that the CAMK2A[p.(Phe98Ser)] and CAMK2A[p.(Glu183Val)] variants result in a dominant acting loss of function (LoF) of the protein, whereas CAMK2A[p.(Glu109Asp)] and CAMK2A[p.(His282Arg)] induce a dominant acting gain of function (GoF). Surprisingly, the CAMK2A[p.(Thr286Pro)] variant, which cannot be auto-phosphorylated at Thr286, behaves as a dominant acting GoF mutation. For CAMK2A[p.(Pro138Ala)], CAMK2A[p.(Pro212Leu)], or CAMK2A[p.(Pro235Leu)], we found minimal effect on stability, autophosphorylation, and neuronal migration; thus, the pathogenicity of these variants by functional assay cannot be definitively confirmed. However, they likely affect other aspects of CAMK2 and neuronal function that were not examined in this study. For instance, the CAMK2A[p.(Pro212Leu)] variant recurs in three individuals

with similar phenotypes, is located in the most missense depleted sequence of CAMK2A (Figure S10), and does not appear in large variant databases like ExAC or gnomAD, which is consistent with pathogenicity. This example underscores the necessity of designing additional tests to assess the effects of variants that could not be confidently classified by our screening.

We found that increased as well as decreased levels of CAMK2B during neuronal development caused migration defects, indicating that cortical development requires an optimal amount of CAMK2B protein. Of the four tested missense variants in CAMK2B, we found that CAMK2B[p.(Lys301Glu)] acts as a LoF mutation, showing reduced phosphorylation of Thr287 with less impaired migration compared to increased levels of CAMK2B[WT]. In contrast, increased Thr287 phosphorylation severely affected neuronal migration (compared to CAMK2B[WT]), suggesting that CAMK2B[p.(Glu110Lys)], CAMK2B[p.(Pro139Leu)], and CAMK2B[p.(Glu237Lys)] act as GoF mutations. Taken
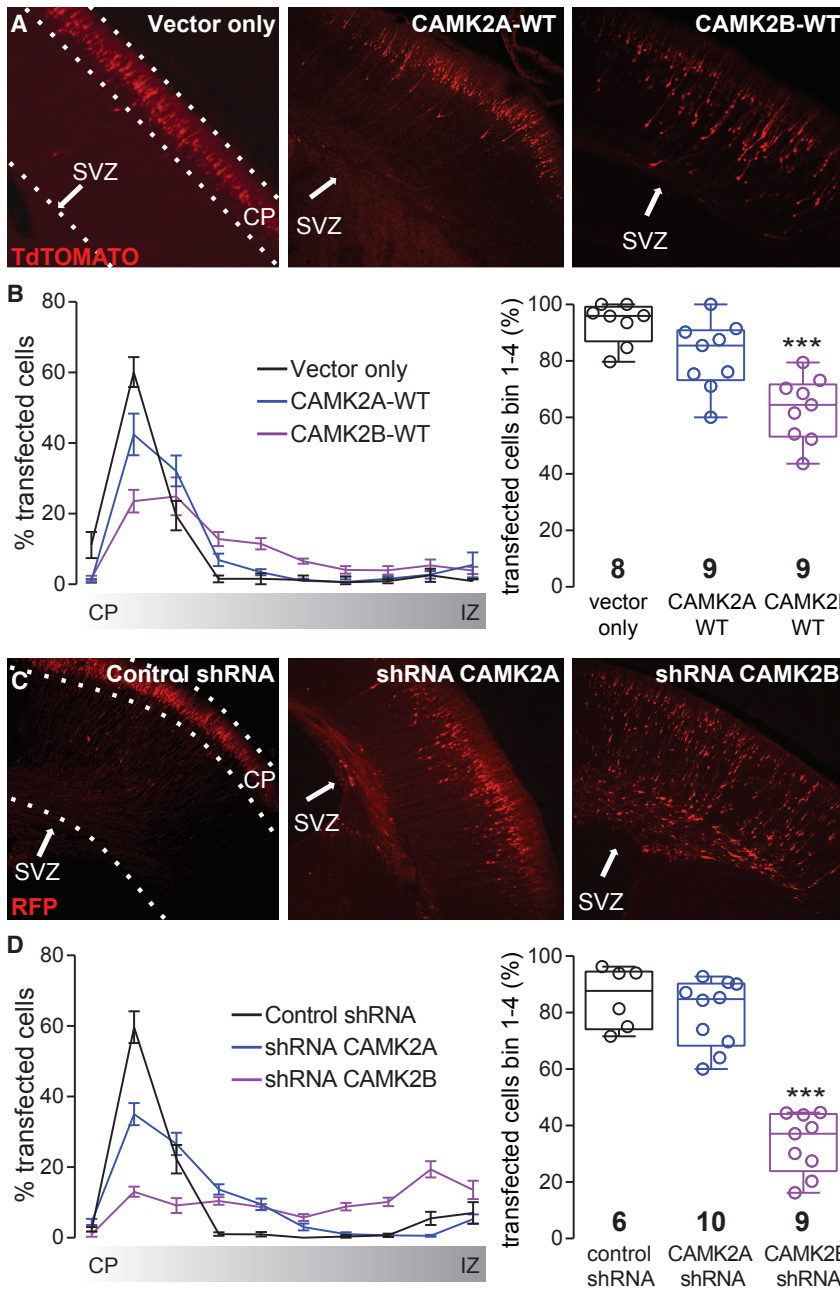
Figure 3. Increased or Decreased Levels of the CAMK2B but Not the CAMK2A Protein *In Vivo* Cause Deficits in Neuronal Migration in Mice

(A) Representative images of E14.5 *in utero* electroporated P0 brains (overexpression of CAMK2), with the cortical plate (CP, dashed lines) and the subventricular zone (SVZ, arrow) indicated. tdTomato-positive cells represent the successfully transfected neurons.

(B) Left: Quantification of the neuronal migration pattern observed in the different conditions. The cortex was divided into 10 bins of equal size and the percentage of tdTomato$^+$/RFP$^+$ cells per bin was counted. Right: Analysis of the percentage of targeted cells that reach the outer layers of the cortex measured as the sum of bin 1 to 4.

(C) Representative images of E14.5 *in utero* electroporated P0 brains (knockdown of endogenous CAMK2), with the cortical plate (CP, dashed lines) and the subventricular zone (SVZ, arrow) indicated. RFP-positive cells represent the successfully transfected neurons.

(D) Left: Quantification of the neuronal migration pattern observed in the different conditions. The cortex was divided into 10 bins of equal size and the percentage of tdTomato$^+$/RFP$^+$ cells per bin was counted. Right: Analysis of the percentage of targeted cells that reach the outer layers of the cortex measured as the sum of bin 1 to 4.

Number in the box and whisker plot graphs indicates the number of pictures analyzed per construct. Error bars indicate the minimum and maximum of all data. Individual data points are shown in the box and whisker plots.

together, these results indicate that not only LoF but also GoF mutations in *CAMK2B* can disturb neurodevelopment, consistent with the notion that cortical development is highly sensitive to dosage of CAMK2B protein.

Considering that three of the variants, p.His282Arg, p.Thr286Pro, and p.Lys301Glu, are positioned in the regulatory domain, their effect on CAMK2 function could have potentially been predicted *a priori*. The CAMK2A His residue at 282 has been shown to be one of the important amino acid residues for potent inhibition of CAMK2A. Indeed, substitution of the histidine with an alanine at this position reduced the inhibitory potency about 25-fold.[67] This is consistent with our findings of increased Thr286 autophosphorylation found in the CAMK2A$^{p.(His282Arg)}$ mutant. Similarly, the CAMK2A p.Thr286Pro variant blocks the critical Thr286 auto-phosphorylation of CAMK2A and hence is likely to be highly pathogenic. Surprisingly, however, we found that instead of acting as a LoF mutant, the variant renders the CAMK2A protein constitutively active and that silencing the kinase activity of this mutant form of CAMK2A normalizes migration. This is a rather unexpected finding, but one possible explanation could be that the change from a threonine into a proline causes a conformational change that is similar to undergoing phosphorylation at this site or to introducing a negatively charged amino acid.[61,62] Whether this is indeed the case will be subject of future research. Lastly, the CAMK2B p.Lys301Glu variant is located in the Ca^{2+}/Calmodulin (CaM) binding domain of CAMK2B and is therefore likely to interfere with Ca^{2+}/CaM binding and hence its activity. Indeed, our *in vitro* data show that phosphorylation of CAMK2B
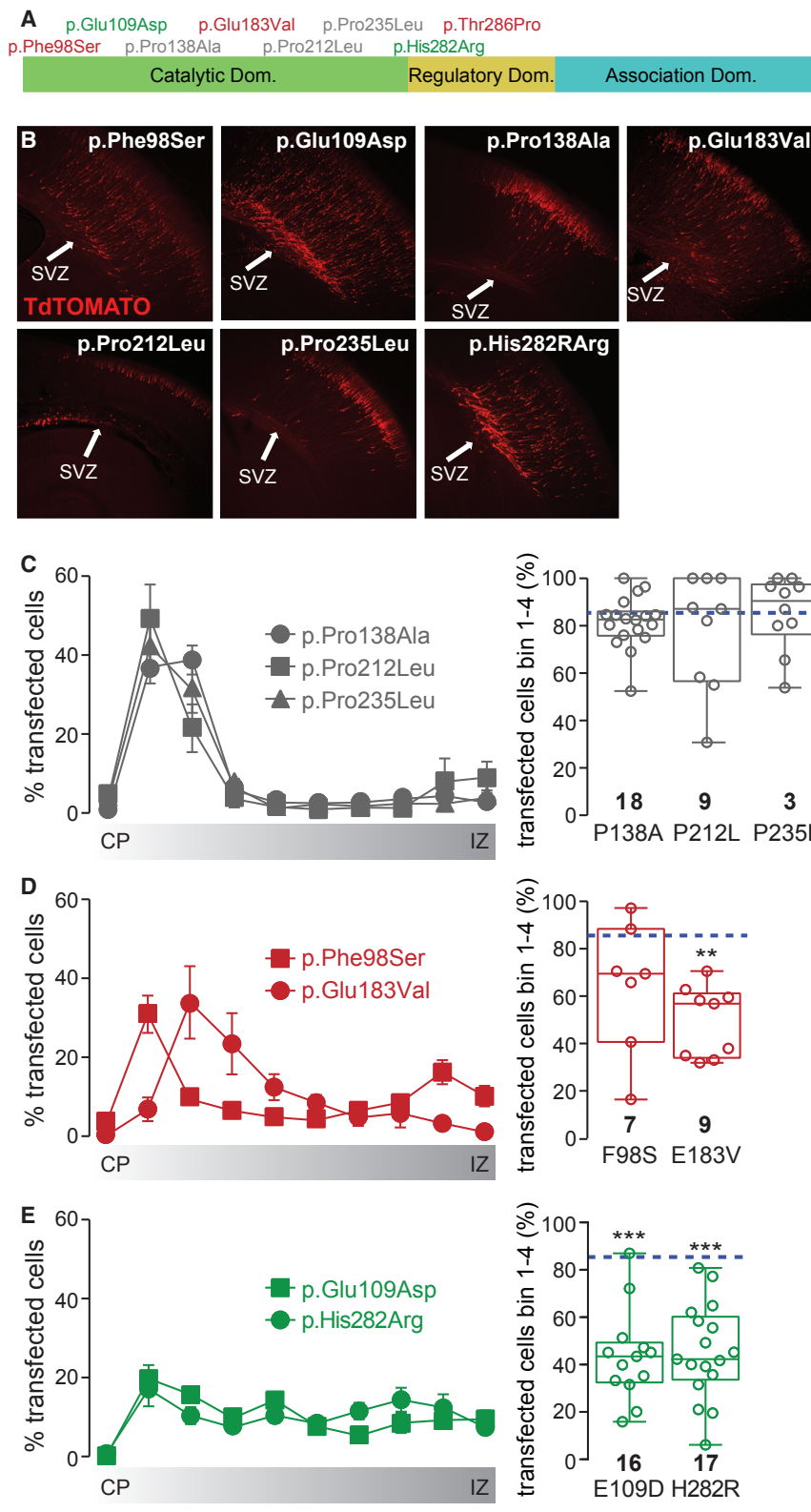
Figure 4. Transfection of CAMK2A Mutations with Changes in Thr286 Phosphorylation In Vivo Induces Migration Deficits

(A) Schematic overview of CAMK2A with the location of the variants with increased (green), decreased (red), or unchanged (gray) Thr286 phosphorylation.

(B) Representative images of E14.5 *in utero* electroporated P0 brains. tdTomato-positive cells represent the successfully transfected neurons.

(C–E) Left: Quantification of the neuronal migration pattern observed in the variants with unchanged (C), decreased (D), or increased (E) Thr286 auto-phosphorylation. Right: Analysis of the percentage of targeted cells of the different constructs that reach the outer layers of the cortex measured as the sum of bin 1 to 4. Dotted line indicates the WT level.

Number in the box and whisker plot graphs indicates the number of pictures analyzed per construct. Error bars indicate the minimum and maximum of all data. Individual data points are shown in the box and whisker plots.

has severe motor deficits[69] but no clear spatial learning or plasticity phenotype.[33] Individual 23, in whom the CAMK2B[p.(Lys301Gly)] variant was identified, also presents the hemizygous variant *NLGN3* (GenBank: NM_018977; c.214dupG; p.Val72Glyfs*17), inherited from his mother who has microcephaly but no other cognitive or developmental impairments. Hence, it is still possible that the combination of both variants resulted in the clinical features.

The remainder of the missense variants found in our cohort all lie in the catalytic domain of the kinase and their effect is harder to predict *a priori*. The CAMK2A p.Glu183Val (CAMK2A[p.(Glu183Val)]) variant was recently published by the Simons Simplex Collection as part of a large cohort study on autism spectrum disorders[38] and studied in a mouse model.[55] In this study, the authors show that the CAMK2A[p.(Glu183Val)] variant results in reduced expression and activity of CAMK2A and causes behavioral deficits.[55] These results are in line with our finding that the variant CAMK2A[p.(Glu183Val)] renders the protein unstable, reduces autonomous activity, and affects neuronal migration. The parallel findings emphasize the usefulness of the assays we employed to assess pathogenicity.

at Thr287 is largely absent. A knock-in mutation in CAMK2A (CAMK2[p.(Thr305Asp)]) that interferes with Ca/CaM binding has a dramatic effect on synaptic plasticity and learning.[27] However, the *Camk2b[p.(Ala303Arg)]* mouse mutant, in which CaM can no longer bind to Camk2b,[68]
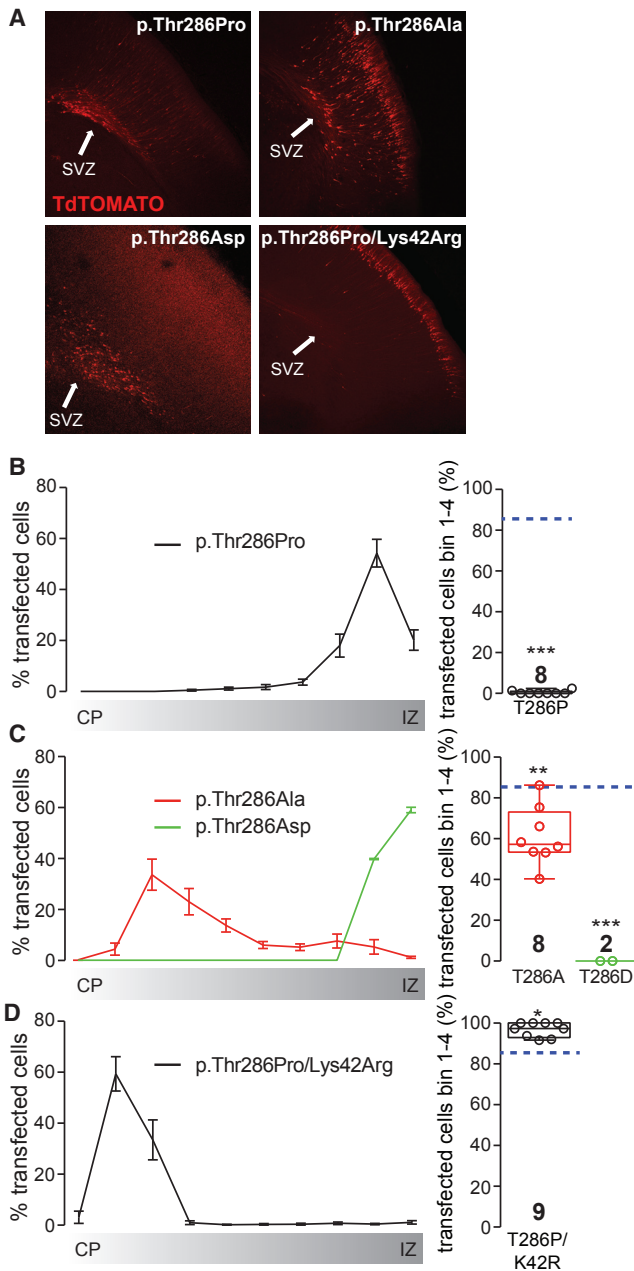
Figure 5. Transfection of the CAMK2A^p.(Thr286Pro) Mutation *In Vivo* Reveals a Constitutive Active Phenotype

(A) Representative images of E14.5 *in utero* electroporated P0 brains. tdTomato-positive cells represent the successfully transfected neurons.

(B) Left: Quantification of the neuronal migration pattern observed when overexpressing CAMK2A^p.(Thr286Pro). Right: Analysis of the percentage of targeted cells of the different constructs that reach the outer layers of the cortex measured as the sum of bin 1 to 4.

(C) Left: Quantification of the neuronal migration pattern observed when overexpressing CAMK2A^p.(Thr286Ala) or CAMK2A^p.(Thr286Pro). Right: Analysis of the percentage of targeted cells of the different constructs that reach the outer layers of the cortex measured as the sum of bin 1 to 4.

(D) Left: Quantification of the neuronal migration pattern observed when overexpressing CAMK2A^p.(Thr286Pro)/p.(Lys42Arg). Right: Analysis of the percentage of targeted cells of the different constructs that reach the outer layers of the cortex measured as the sum of bin 1 to 4. Dotted line indicates the WT level.

We observed that some variants resulted in increased and others in decreased CAMK2 activity and that all such variants also affected neuronal migration. However, the precise underlying pathogenic mechanisms may nevertheless be more complex and require further functional studies. An unresolved issue is whether haploinsufficiency could also lead to the same phenotype, as suggested by frameshift *CAMK2A* c.65del (p.Gly22Glufs*10) and nonsense *CAMK2B* c.85C>T (p.Arg29*) variants and by *CAMK2A* c.1204+1G>A which leads to out-of-frame skipping of exon 17. According to variant databases, *CAMK2A* and *CAMK2B* are predicted to be haploinsufficient (Table S4). Indeed, loss-of-function variants are exceedingly rare, in particular for the most abundant transcripts in brain, which are GenBank: NM_171825.2 for *CAMK2A* and GenBank: NM_172079.2 for *CAMK2B* (Figures S7 and S8). For these two transcripts combined, only three LoF variants were identified in 62,000 exomes sequenced by ExAC, and three in more than 69,500 exomes sequenced by centers participating in the study. A small deletion in 5q32 encompassing *CAMK2A* and four other genes was reported in two case subjects with Treacher Collins syndrome in which ID was suspected to be due to the deletion of *CAMK2A*.[70] The haploinsufficiency hypothesis is consistent with our knockdown experiments that showed that reduced CAMK2B disrupts migration. Yet, given that the amount of protein was reduced to 20%, this experiment may not be an appropriate test for haploinsufficiency. Our migration assay was insensitive to reducing CAMK2A levels, but this is not surprising given that CAMK2A is hardly expressed at this time point. Even if haploinsufficiency accounts for some of the case subjects, it is noteworthy that, *CAMK2A* and *CAMK2B* taken together, the ID seen in individuals included in our study seems more severe when associated with GoF variants (4/5) than when associated with LoF variants (1/6) (Table S2). This is consistent with the rather weak phenotypes of heterozygous *Camk2a* and *Camk2b* knock-out mice,[27,28,30,31,65,71] in contrast with the more severe phenotypes of mice with variants affecting autophosphorylation.

Of note, the case of variant *CAMK2A* c.1204+1G>A contrasts with the other variants in the series, as this is the only variant to interrupt the association domain. A similar observation was made in a recessive form of ID (B. Reversade, personal communication).

Our functional studies highlight the variety of mechanisms leading to ID related to CAMK2A/B mutations. Most certainly, this variety reflects the multiple ways CAMK2 acts on synaptic plasticity.[24] We can therefore postulate that the spectrum of neurological disorders associated with *CAMK2A/B* variants could extend to other rare

Number in the box and whisker plot graphs indicates the number of pictures analyzed per construct. Error bars indicate the minimum and maximum of all data. Individual data points are shown in the box and whisker plots.
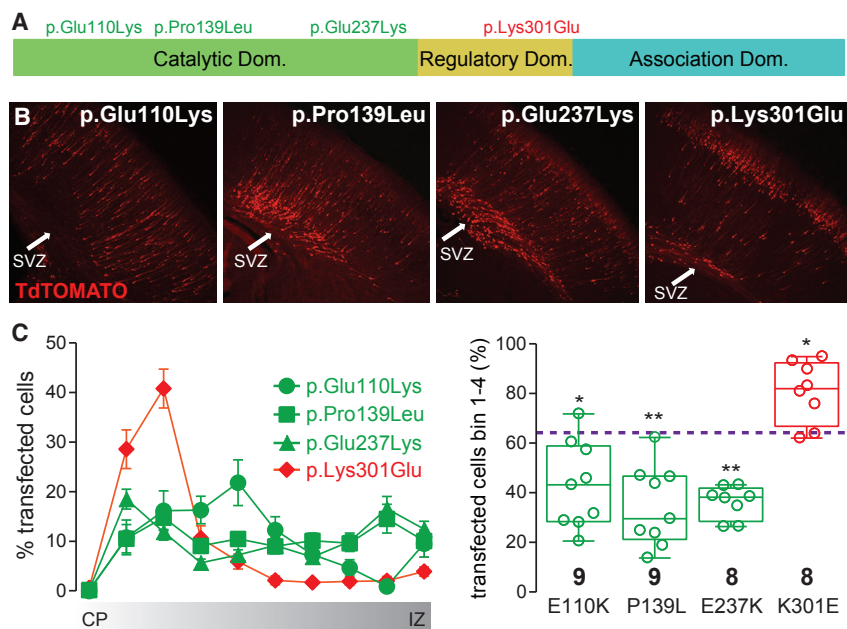
Figure 6. Transfection of CAMK2B Mutations *In Vivo* Causes Changes in the Migration Pattern of the Targeted Neurons

(A) Schematic overview of CAMK2B with the location of the mutations with increased (green), decreased (red), or unchanged (gray) Thr286 phosphorylation.

(B) Representative images of E14.5 *in utero* electroporated P0 brains. tdTomato-positive cells represent the successfully transfected neurons.

(C) Left: Quantification of the neuronal migration pattern observed when overexpressing the mutations. Right: Analysis of the percentage of targeted cells of the different constructs that reach the outer layers of the cortex measured as the sum of bin 1 to 4. Dotted line indicates the WT level.

Number in the box and whisker plot graph indicates the number of pictures analyzed per construct. Error bars indicate the minimum and maximum of all data. Individual data points are shown in the box and whisker plots.

or common neurological or psychiatric disorders, as already suggested by others.[72] In our series, we stressed the frequency of abnormal behaviors, which is in line with a previous study suggesting a relationship between *CAMK2A* mutations and autism spectrum disorder.[55] *CAMK2A* involvement was also recently shown in bipolar disorders.[73] Given their tight link in NMDA-dependent LTP process, it is very tempting to draw a comparison between *CAMK2* and *GRIN2B* or *GRIN2A*. Variants in the latter genes may cause ID[17,74,75] and infantile epileptic encephalopathy,[18] epileptic aphasia,[20] or be associated with Tourette syndrome,[76] schizophrenia,[77] or autism.[78]

In conclusion, our observations highlight a rare genetic cause of developmental delay/ID due to alterations in genes encoding subunits of CAMK2, a key holoenzyme in learning and memory processes in the AMPAR- and NMDAR-dependent signaling pathways. Our findings expand the phenotypic spectrum of the disorders caused by variants in other key actors of this pathway. We have identified mutations in two *CAMK2* paralogous genes as the cause of a neurodevelopmental phenotype characterized by ID. Functional studies performed in this study suggest that *CAMK2A* and *CAMK2B* may be involved in a broad range of neurologic and psychiatric disorders.

Accession Numbers

The sequence variants reported in the paper have been deposited in ClinVar database (SCV000583477 to SCV000583493) and in the Leiden Open Variation Database under accession numbers #0000172749, #0000172803, #0000172804, #0000172805, #0000172806, #0000172807, #0000172808, #0000172814, #0000172880, #0000172881, #0000172882, #0000172884, #0000222042, and #0000222044 for CAMK2A, and under accession numbers #0000172887, #0000172888, #0000172889, #0000172890, #0000172891, #0000172892, #0000172893, #0000172894, and #0000172895 for CAMK2B. Correspondences between variants and accession numbers are indicated in Table S1.

Exome-sequencing and phenotype data from Deciphering Developmental Disorders (individuals 3, 14, 18 and 21) are accessible via the European Genome-phenome Archive (EGA) under accession number EGAS00001000775.

Sequence data from Simons Simplex Collection (individuals 5 and 6) used in these work are available from the National Database for Autism Research under study DOI: 10.15154/1149697.

Data from Boston Children's Hospital (USA; individual 17) available with Gene Discovery Core, Manton Center for Orphan Disease Research.

The *CAMK2A* variant c.635C>T (p.Pro212Leu) for individual 9 is also deposited in DECIPHER (accession number 332886). The *CAMK2A* variant c.704C>T (p.Pro235Leu) for individual 10 had been submitted to ClinVar under accession number SCV000258098 and was assigned a dbSNP number rs864309606 thereafter.

Exome-sequencing data from the following institutions have not been deposited because participating individuals have not consented for the data to be publicly released: Baylor Genetics (BG) Laboratories (individuals 1 and 16), HUGODIMS project (individuals 2 and 7), University Medical Center Utrecht (individuals 4 and 12), University Hospital Center (CHU) of Lyon (individual 8), Leiden University Medical Center (individual 9), Children's Hospital of Philadelphia (individual 10), Institute of Human Genetics Heidelberg (individual 11), GeneDx laboratory (individuals 13, 15, 19 and 22), Boston Children's Hospital/UDN (individual 20), and University of Illinois College of Medicine at Peoria via Ambry Genetics (individual 23, Telemark Hospital in Skien (individual 24).

Supplemental Data

Supplemental Data include ten figures, four tables, Supplemental Acknowledgments, and Supplemental Note (on clinical cases) and can be found with this article online at https://doi.org/10.1016/j.ajhg.2017.10.003.

Web Resources

1000 Genomes, http://www.internationalgenome.org/
CADD, http://cadd.gs.washington.edu/
ClinVar, https://www.ncbi.nlm.nih.gov/clinvar/
Clustal Omega, https://www.ebi.ac.uk/Tools/msa/clustalo/
dbSNP, https://www.ncbi.nlm.nih.gov/projects/SNP/
DECIPHER, https://decipher.sanger.ac.uk/
DiscovEHR, http://www.discovehrshare.com/
European Genome-phenome Archive (EGA), https://www.ebi.ac.uk/ega/studies/EGAS00001000775
ExAC Browser, http://exac.broadinstitute.org/
GATK, https://software.broadinstitute.org/gatk/
GenBank, https://www.ncbi.nlm.nih.gov/genbank/
GeneMatcher, https://genematcher.org/
Genic Intolerance, http://genic-intolerance.org/
gnomAD Browser, http://gnomad.broadinstitute.org/
GoNL (Genomes of the Netherlands), http://www.nlgenome.nl/search/
GTEx Portal, https://www.gtexportal.org/home/
HBT – Human Brain Transcriptome, http://hbatlas.org/
I-TASSER, https://zhanglab.ccmb.med.umich.edu/I-TASSER/
JVarkit, https://doi.org/10.6084/m9.figshare.1425030/
LOVD for CAMK2A, http://databases.lovd.nl/shared/genes/CAMK2A
LOVD for CAMK2B, http://databases.lovd.nl/shared/genes/CAMK2B
MAP 2 Ref, http://www.sysy.com/products/map2/ref.php
Missense Tolerance Ratio (MTR), http://mtr-viewer.mdhs.unimelb.edu.au/
MutationTaster, http://www.mutationtaster.org/
National Database for Autism Research, https://ndar.nih.gov
NHLBI Exome Sequencing Project (ESP) Exome Variant Server, http://evs.gs.washington.edu/EVS/
OMIM, http://www.omim.org/
Picard, http://broadinstitute.github.io/picard/
PLINK 1.9, https://www.cog-genomics.org/plink2/
PolyPhen-2, http://genetics.bwh.harvard.edu/pph2/
Primer3Plus, http://www.primer3plus.com/cgi-bin/dev/primer3plus.cgi
PyMOL, http://www.pymol.org
RCSB Protein Data Bank, http://www.rcsb.org/pdb/home/home.do
SAMtools, http://samtools.sourceforge.net/
SIFT Human Protein, http://www.jcvi.org/www/SIFT_enst_submit.html
SnpEff, http://snpeff.sourceforge.net/
The Human Protein Atlas, http://www.proteinatlas.org/tissue
UCSC Genome Browser, http://genome.ucsc.edu
wANNOVAR, http://wannovar.wglab.org/

References

1. Grant, S.G., and Silva, A.J. (1994). Targeting learning. Trends Neurosci. *17*, 71–75.
2. Lisman, J., Yasuda, R., and Raghavachari, S. (2012). Mechanisms of CaMKII action in long-term potentiation. Nat. Rev. Neurosci. *13*, 169–182.
3. Fan, X., Jin, W.Y., and Wang, Y.T. (2014). The NMDA receptor complex: a multifunctional machine at the glutamatergic synapse. Front. Cell. Neurosci. *8*, 160.
4. Malenka, R.C., and Bear, M.F. (2004). LTP and LTD: an embarrassment of riches. Neuron *44*, 5–21.
5. Buffington, S.A., Huang, W., and Costa-Mattioli, M. (2014). Translational control in synaptic plasticity and cognitive dysfunction. Annu. Rev. Neurosci. *37*, 17–38.
6. Bliss, T.V., Collingridge, G.L., and Morris, R.G. (2013). Synaptic plasticity in health and disease: introduction and overview. Philos. Trans. R. Soc. Lond. B Biol. Sci. *369*, 20130129.
7. Lau, C.G., and Zukin, R.S. (2007). NMDA receptor trafficking in synaptic plasticity and neuropsychiatric disorders. Nat. Rev. Neurosci. *8*, 413–426.
8. Mony, L., Kew, J.N., Gunthorpe, M.J., and Paoletti, P. (2009). Allosteric modulators of NR2B-containing NMDA receptors: molecular mechanisms and therapeutic potential. Br. J. Pharmacol. *157*, 1301–1317.
9. Traynelis, S.F., Wollmuth, L.P., McBain, C.J., Menniti, F.S., Vance, K.M., Ogden, K.K., Hansen, K.B., Yuan, H., Myers, S.J., and Dingledine, R. (2010). Glutamate receptor ion channels: structure, regulation, and function. Pharmacol. Rev. *62*, 405–496.
10. Barkus, C., Sanderson, D.J., Rawlins, J.N., Walton, M.E., Harrison, P.J., and Bannerman, D.M. (2014). What causes aberrant salience in schizophrenia? A role for impaired short-term habituation and the GRIA1 (GluA1) AMPA receptor subunit. Mol. Psychiatry *19*, 1060–1070.
11. Zhang, J., and Abdullah, J.M. (2013). The role of GluA1 in central nervous system disorders. Rev. Neurosci. *24*, 499–505.
12. Wu, Y., Arai, A.C., Rumbaugh, G., Srivastava, A.K., Turner, G., Hayashi, T., Suzuki, E., Jiang, Y., Zhang, L., Rodriguez, J., et al. (2007). Mutations in ionotropic AMPA receptor 3 alter channel properties and are associated with moderate cognitive impairment in humans. Proc. Natl. Acad. Sci. USA *104*, 18163–18168.
13. Philips, A.K., Sirén, A., Avela, K., Somer, M., Peippo, M., Ahvenainen, M., Doagu, F., Arvio, M., Kääriäinen, H., Van Esch, H., et al. (2014). X-exome sequencing in Finnish families with intellectual disability–four novel mutations and two novel syndromic phenotypes. Orphanet J. Rare Dis. *9*, 49.
14. Hamdan, F.F., Gauthier, J., Araki, Y., Lin, D.T., Yoshizawa, Y., Higashi, K., Park, A.R., Spiegelman, D., Dobrzeniecka, S., Piton, A., et al.; S2D Group (2011). Excess of de novo deleterious mutations in genes associated with glutamatergic systems in nonsyndromic intellectual disability. Am. J. Hum. Genet. *88*, 306–316.
15. Li, D., Yuan, H., Ortiz-Gonzalez, X.R., Marsh, E.D., Tian, L., McCormick, E.M., Kosobucki, G.J., Chen, W., Schulien, A.J., Chiavacci, R., et al. (2016). GRIN2D recurrent de novo dominant mutation causes a severe epileptic encephalopathy treatable with NMDA receptor channel blockers. Am. J. Hum. Genet. *99*, 802–816.
16. Carvill, G.L., Regan, B.M., Yendle, S.C., O'Roak, B.J., Lozovaya, N., Bruneau, N., Burnashev, N., Khan, A., Cook, J., Geraghty, E., et al. (2013). GRIN2A mutations cause epilepsy-aphasia spectrum disorders. Nat. Genet. *45*, 1073–1076.
17. Endele, S., Rosenberger, G., Geider, K., Popp, B., Tamer, C., Stefanova, I., Milh, M., Kortüm, F., Fritsch, A., Pientka, F.K., et al. (2010). Mutations in GRIN2A and GRIN2B encoding regulatory subunits of NMDA receptors cause variable neurodevelopmental phenotypes. Nat. Genet. *42*, 1021–1026.

18. Lemke, J.R., Hendrickx, R., Geider, K., Laube, B., Schwake, M., Harvey, R.J., James, V.M., Pepler, A., Steiner, I., Hörtnagel, K., et al. (2014). GRIN2B mutations in West syndrome and intellectual disability with focal epilepsy. Ann. Neurol. *75*, 147–154.

19. Lemke, J.R., Lal, D., Reinthaler, E.M., Steiner, I., Nothnagel, M., Alber, M., Geider, K., Laube, B., Schwake, M., Finsterwalder, K., et al. (2013). Mutations in GRIN2A cause idiopathic focal epilepsy with rolandic spikes. Nat. Genet. *45*, 1067–1072.

20. Lesca, G., Rudolf, G., Bruneau, N., Lozovaya, N., Labalme, A., Boutry-Kryza, N., Salmi, M., Tsintsadze, T., Addis, L., Motte, J., et al. (2013). GRIN2A mutations in acquired epileptic aphasia and related childhood focal epilepsies and encephalopathies with speech and language dysfunction. Nat. Genet. *45*, 1061–1066.

21. Lisman, J., Schulman, H., and Cline, H. (2002). The molecular basis of CaMKII function in synaptic and behavioural memory. Nat. Rev. Neurosci. *3*, 175–190.

22. Erondu, N.E., and Kennedy, M.B. (1985). Regional distribution of type II Ca2+/calmodulin-dependent protein kinase in rat brain. J. Neurosci. *5*, 3270–3277.

23. Colbran, R.J. (2004). Targeting of calcium/calmodulin-dependent protein kinase II. Biochem. J. *378*, 1–16.

24. Kim, K., Saneyoshi, T., Hosokawa, T., Okamoto, K., and Hayashi, Y. (2016). Interplay of enzymatic and structural functions of CaMKII in long-term potentiation. J. Neurochem. *139*, 959–972.

25. Paoletti, P., Bellone, C., and Zhou, Q. (2013). NMDA receptor subunit diversity: impact on receptor properties, synaptic plasticity and disease. Nat. Rev. Neurosci. *14*, 383–400.

26. Hoffman, L., Farley, M.M., and Waxham, M.N. (2013). Calcium-calmodulin-dependent protein kinase II isoforms differentially impact the dynamics and structure of the actin cytoskeleton. Biochemistry *52*, 1198–1207.

27. Elgersma, Y., Fedorov, N.B., Ikonen, S., Choi, E.S., Elgersma, M., Carvalho, O.M., Giese, K.P., and Silva, A.J. (2002). Inhibitory autophosphorylation of CaMKII controls PSD association, plasticity, and learning. Neuron *36*, 493–505.

28. Giese, K.P., Fedorov, N.B., Filipkowski, R.K., and Silva, A.J. (1998). Autophosphorylation at Thr286 of the alpha calcium-calmodulin kinase II in LTP and learning. Science *279*, 870–873.

29. Yamagata, Y., Kobayashi, S., Umeda, T., Inoue, A., Sakagami, H., Fukaya, M., Watanabe, M., Hatanaka, N., Totsuka, M., Yagi, T., et al. (2009). Kinase-dead knock-in mouse reveals an essential role of kinase activity of Ca2+/calmodulin-dependent protein kinase IIalpha in dendritic spine enlargement, long-term potentiation, and learning. J. Neurosci. *29*, 7607–7618.

30. Silva, A.J., Stevens, C.F., Tonegawa, S., and Wang, Y. (1992). Deficient hippocampal long-term potentiation in alpha-calcium-calmodulin kinase II mutant mice. Science *257*, 201–206.

31. Silva, A.J., Paylor, R., Wehner, J.M., and Tonegawa, S. (1992). Impaired spatial learning in alpha-calcium-calmodulin kinase II mutant mice. Science *257*, 206–211.

32. van Woerden, G.M., Hoebeek, F.E., Gao, Z., Nagaraja, R.Y., Hoogenraad, C.C., Kushner, S.A., Hansel, C., De Zeeuw, C.I., and Elgersma, Y. (2009). betaCaMKII controls the direction of plasticity at parallel fiber-Purkinje cell synapses. Nat. Neurosci. *12*, 823–825.

33. Borgesius, N.Z., van Woerden, G.M., Buitendijk, G.H., Keijzer, N., Jaarsma, D., Hoogenraad, C.C., and Elgersma, Y. (2011). βCaMKII plays a nonenzymatic role in hippocampal synaptic plasticity and learning by targeting αCaMKII to synapses. J. Neurosci. *31*, 10141–10148.

34. Sobreira, N., Schiettecatte, F., Valle, D., and Hamosh, A. (2015). GeneMatcher: a matching tool for connecting investigators with an interest in the same gene. Hum. Mutat. *36*, 928–930.

35. Firth, H.V., Richards, S.M., Bevan, A.P., Clayton, S., Corpas, M., Rajan, D., Van Vooren, S., Moreau, Y., Pettett, R.M., and Carter, N.P. (2009). DECIPHER: Database of Chromosomal Imbalance and Phenotype in Humans Using Ensembl Resources. Am. J. Hum. Genet. *84*, 524–533.

36. Isidor, B., Küry, S., Rosenfeld, J.A., Besnard, T., Schmitt, S., Joss, S., Davies, S.J., Lebel, R.R., Henderson, A., Schaaf, C.P., et al. (2016). De novo truncating mutations in the kinetochore-microtubules attachment gene CHAMP1 cause syndromic intellectual disability. Hum. Mutat. *37*, 354–358.

37. Deciphering Developmental Disorders, S.; and Deciphering Developmental Disorders Study (2017). Prevalence and architecture of de novo mutations in developmental disorders. Nature *542*, 433–438.

38. Iossifov, I., O'Roak, B.J., Sanders, S.J., Ronemus, M., Krumm, N., Levy, D., Stessman, H.A., Witherspoon, K.T., Vives, L., Patterson, K.E., et al. (2014). The contribution of de novo coding mutations to autism spectrum disorder. Nature *515*, 216–221.

39. Retterer, K., Juusola, J., Cho, M.T., Vitazka, P., Millan, F., Gibellini, F., Vertino-Bell, A., Smaoui, N., Neidich, J., Monaghan, K.G., et al. (2016). Clinical application of whole-exome sequencing across clinical indications. Genet. Med. *18*, 696–704.

40. Brownstein, C.A., Beggs, A.H., Rodan, L., Shi, J., Towne, M.C., Pelletier, R., Cao, S., Rosenberg, P.A., Urion, D.K., Picker, J., et al. (2016). Clinical heterogeneity associated with KCNA1 mutations include cataplexy and nonataxic presentations. Neurogenetics *17*, 11–16.

41. Nesbitt, A., Bhoj, E.J., McDonald Gibson, K., Yu, Z., Denenberg, E., Sarmady, M., Tischler, T., Cao, K., Dubbs, H., Zackai, E.H., and Santani, A. (2015). Exome sequencing expands the mechanism of SOX5-associated intellectual disability: A case presentation with review of sox-related disorders. Am. J. Med. Genet. A. *167A*, 2548–2554.

42. Farwell, K.D., Shahmirzadi, L., El-Khechen, D., Powis, Z., Chao, E.C., Tippin Davis, B., Baxter, R.M., Zeng, W., Mroske, C., Parra, M.C., et al. (2015). Enhanced utility of family-centered diagnostic exome sequencing with inheritance model-based analysis: results from 500 unselected families with undiagnosed genetic conditions. Genet. Med. *17*, 578–586.

43. Hempel, M., Cremer, K., Ockeloen, C.W., Lichtenbelt, K.D., Herkert, J.C., Denecke, J., Haack, T.B., Zink, A.M., Becker, J., Wohlleber, E., et al. (2015). De novo mutations in CHAMP1 cause intellectual disability with severe speech impairment. Am. J. Hum. Genet. *97*, 493–500.

44. Holla, O.L., Busk, O.L., Tveten, K., Hilmarsen, H.T., Strand, L., Høyer, H., Bakken, A., Skjelbred, C.F., and Braathen, G.J. (2015). Clinical exome sequencing – Norwegian findings. Tidsskr. Nor. Laegeforen. *135*, 1833–1837.

45. Santen, G.W., Aten, E., Sun, Y., Almomani, R., Gilissen, C., Nielsen, M., Kant, S.G., Snoeck, I.N., Peeters, E.A., Hilhorst-Hofstee, Y., et al. (2012). Mutations in SWI/SNF chromatin

remodeling complex gene ARID1B cause Coffin-Siris syndrome. Nat. Genet. *44*, 379–380.

46. Bainbridge, M.N., Wang, M., Wu, Y., Newsham, I., Muzny, D.M., Jefferies, J.L., Albert, T.J., Burgess, D.L., and Gibbs, R.A. (2011). Targeted enrichment beyond the consensus coding DNA sequence exome reveals exons with higher variant densities. Genome Biol. *12*, R68.

47. Yang, Y., Muzny, D.M., Reid, J.G., Bainbridge, M.N., Willis, A., Ward, P.A., Braxton, A., Beuten, J., Xia, F., Niu, Z., et al. (2013). Clinical whole-exome sequencing for the diagnosis of mendelian disorders. N. Engl. J. Med. *369*, 1502–1511.

48. Evers, C., Staufner, C., Granzow, M., Paramasivam, N., Hinderhofer, K., Kaufmann, L., Fischer, C., Thiel, C., Opladen, T., Kotzaeridou, U., et al. (2017). Impact of clinical exomes in neurodevelopmental and neurometabolic disorders. Mol. Genet. Metab. *121*, 297–307.

49. van Woerden, G.M., Harris, K.D., Hojjati, M.R., Gustin, R.M., Qiu, S., de Avila Freire, R., Jiang, Y.H., Elgersma, Y., and Weeber, E.J. (2007). Rescue of neurological deficits in a mouse model for Angelman syndrome by reduction of alphaCaMKII inhibitory phosphorylation. Nat. Neurosci. *10*, 280–282.

50. Banker, G., and Goslin, K. (1991). Culturing Nerve Cells (Cambridge, MA: MIT Press).

51. Zhang, Y. (2008). I-TASSER server for protein 3D structure prediction. BMC Bioinformatics *9*, 40.

52. Deciphering Developmental Disorders Study (2015). Large-scale discovery of novel genetic causes of developmental disorders. Nature *519*, 223–228.

53. Ware, J.S., Samocha, K.E., Homsy, J., and Daly, M.J. (2015). Interpreting de novo variation in human disease using denovolyzeR. Current Prot. Human Genet. *87*, 21–15.

54. Traynelis, J., Silk, M., Wang, Q., Berkovic, S.F., Liu, L., Ascher, D.B., Balding, D.J., and Petrovski, S. (2017). Optimizing genomic medicine in epilepsy through a gene-customized approach to missense variant interpretation. Genome Res. *27*, 1715–1729.

55. Stephenson, J.R., Wang, X., Perfitt, T.L., Parrish, W.P., Shonesy, B.C., Marks, C.R., Mortlock, D.P., Nakagawa, T., Sutcliffe, J.S., and Colbran, R.J. (2017). A novel human CAMK2A mutation disrupts dendritic morphology and synaptic transmission, and causes ASD-related behaviors. J. Neurosci. *37*, 2216–2233.

56. Tabata, H., and Nakajima, K. (2001). Efficient in utero gene transfer system to the developing mouse brain using electroporation: visualization of neuronal migration in the developing cortex. Neuroscience *103*, 865–872.

57. Saito, T., and Nakatsuji, N. (2001). Efficient gene transfer into the embryonic mouse brain using in vivo electroporation. Dev. Biol. *240*, 237–246.

58. Taniguchi, Y., Young-Pearse, T., Sawa, A., and Kamiya, A. (2012). In utero electroporation as a tool for genetic manipulation in vivo to study psychiatric disorders: from genes to circuits and behaviors. Neuroscientist *18*, 169–179.

59. Shen, K., Teruel, M.N., Subramanian, K., and Meyer, T. (1998). CaMKIIbeta functions as an F-actin targeting module that localizes CaMKIIalpha/beta heterooligomers to dendritic spines. Neuron *21*, 593–606.

60. Bayer, K.U., Löhler, J., Schulman, H., and Harbers, K. (1999). Developmental expression of the CaM kinase II isoforms: ubiquitous gamma- and delta-CaM kinase II are the early iso-

forms and most abundant in the developing nervous system. Brain Res. Mol. Brain Res. *70*, 147–154.

61. Mayford, M., Bach, M.E., Huang, Y.Y., Wang, L., Hawkins, R.D., and Kandel, E.R. (1996). Control of memory formation through regulated expression of a CaMKII transgene. Science *274*, 1678–1683.

62. Mayford, M., Wang, J., Kandel, E.R., and O'Dell, T.J. (1995). CaMKII regulates the frequency-response function of hippocampal synapses for the production of both LTD and LTP. Cell *81*, 891–904.

63. Hell, J.W. (2014). CaMKII: claiming center stage in postsynaptic function and organization. Neuron *81*, 249–265.

64. Achterberg, K.G., Buitendijk, G.H., Kool, M.J., Goorden, S.M., Post, L., Slump, D.E., Silva, A.J., van Woerden, G.M., Kushner, S.A., and Elgersma, Y. (2014). Temporal and region-specific requirements of αCaMKII in spatial and contextual learning. J. Neurosci. *34*, 11180–11187.

65. Bachstetter, A.D., Webster, S.J., Tu, T., Goulding, D.S., Haiech, J., Watterson, D.M., and Van Eldik, L.J. (2014). Generation and behavior characterization of CaMKIIβ knockout mice. PLoS ONE *9*, e105191.

66. Barcomb, K., Hell, J.W., Benke, T.A., and Bayer, K.U. (2016). The CaMKII/GluN2B protein interaction maintains synaptic strength. J. Biol. Chem. *291*, 16082–16089.

67. Smith, M.K., Colbran, R.J., Brickey, D.A., and Soderling, T.R. (1992). Functional determinants in the autoinhibitory domain of calcium/calmodulin-dependent protein kinase II. Role of His282 and multiple basic residues. J. Biol. Chem. *267*, 1761–1768.

68. Shen, K., and Meyer, T. (1999). Dynamic control of CaMKII translocation and localization in hippocampal neurons by NMDA receptor stimulation. Science *284*, 162–166.

69. Kool, M.J., van de Bree, J.E., Bodde, H.E., Elgersma, Y., and van Woerden, G.M. (2016). The molecular, temporal and region-specific requirements of the beta isoform of Calcium/Calmodulin-dependent protein kinase type 2 (CAMK2B) in mouse locomotion. Sci. Rep. *6*, 26989.

70. Vincent, M., Collet, C., Verloes, A., Lambert, L., Herlin, C., Blanchet, C., Sanchez, E., Drunat, S., Vigneron, J., Laplanche, J.L., et al. (2014). Large deletions encompassing the TCOF1 and CAMK2A genes are responsible for Treacher Collins syndrome with intellectual disability. Eur. J. Hum. Genet. *22*, 52–56.

71. Chen, C., Rainnie, D.G., Greene, R.W., and Tonegawa, S. (1994). Abnormal fear response and aggressive behavior in mutant mice deficient for alpha-calcium-calmodulin kinase II. Science *266*, 291–294.

72. Takemoto-Kimura, S., Suzuki, K., Horigane, S.I., Kamijo, S., Inoue, M., Sakamoto, M., Fujii, H., and Bito, H. (2017). Calmodulin kinases: essential regulators in health and disease. J. Neurochem. *141*, 808–818.

73. Ament, S.A., Szelinger, S., Glusman, G., Ashworth, J., Hou, L., Akula, N., Shekhtman, T., Badner, J.A., Brunkow, M.E., Mauldin, D.E., et al.; Bipolar Genome Study (2015). Rare variants in neuronal excitability genes influence risk for bipolar disorder. Proc. Natl. Acad. Sci. USA *112*, 3576–3581.

74. O'Roak, B.J., Vives, L., Fu, W., Egertson, J.D., Stanaway, I.B., Phelps, I.G., Carvill, G., Kumar, A., Lee, C., Ankenman, K., et al. (2012). Multiplex targeted sequencing identifies recurrently mutated genes in autism spectrum disorders. Science *338*, 1619–1622.

75. de Ligt, J., Willemsen, M.H., van Bon, B.W., Kleefstra, T., Yntema, H.G., Kroes, T., Vulto-van Silfhout, A.T., Koolen, D.A., de Vries, P., Gilissen, C., et al. (2012). Diagnostic exome sequencing in persons with severe intellectual disability. N. Engl. J. Med. 367, 1921–1929.

76. Che, F., Zhang, Y., Wang, G., Heng, X., Liu, S., and Du, Y. (2015). The role of GRIN2B in Tourette syndrome: Results from a transmission disequilibrium study. J. Affect. Disord. 187, 62–65.

77. Yang, Y., Li, W., Zhang, H., Yang, G., Wang, X., Ding, M., Jiang, T., and Lv, L. (2015). Association study of N-methyl-D-aspartate receptor subunit 2B (GRIN2B) polymorphisms and schizophrenia symptoms in the Han Chinese population. PLoS ONE 10, e0125925.

78. Pan, Y., Chen, J., Guo, H., Ou, J., Peng, Y., Liu, Q., Shen, Y., Shi, L., Liu, Y., Xiong, Z., et al. (2015). Association of genetic variants of GRIN2B with autism. Sci. Rep. 5, 8296.